Neuronal hyperexcitability is a DLK-dependent trigger of HSV-1 reactivation that can be induced by IL-1

Sean Cuddy[1,2#], Austin R. Schinlever[1#], Sara Dochnal[1], Jon Suzich[1], Parijat Kundu[1], Taylor K. Downs[3], Mina Farah[1], Bimal Desai[3], Chris Boutell[4] and Anna R. Cliffe[1*]

1. Department of Microbiology, Immunology and Cancer Biology, University of Virginia, Charlottesville, VA, 22908.
2. Neuroscience Graduate Program, University of Virginia, Charlottesville, VA, 22908
3. Department of Pharmacology, University of Virginia, Charlottesville, VA, 22908.
4. MRC-University of Glasgow Centre for Virus Research (CVR), Garscube Campus, Glasgow, Scotland, United Kingdom

# Denotes equal contribution

* Correspondence to Anna R. Cliffe, cliffe@virginia.edu

Abstract

Herpes Simplex Virus (HSV) establishes a latent infection in neurons and periodically reactivates to cause recurrent disease. The stimuli that act on neurons to trigger HSV reactivation have not been fully elucidated. Here we demonstrate that HSV reactivation is triggered by stimuli that induce neuronal hyperexcitability. Neuronal stimulation-induced reactivation was dependent on voltage-gated ion and hyperpolarization-activated cyclic nucleotide-gated (HCN) channels, demonstrating that neuronal activity is required for HSV reactivation. Hyperexcitability-induced reactivation was dependent on the neuronal specific pathway of DLK/JNK activation and progressed via an initial wave of viral gene expression that was independent of histone demethylase activity and linked to increased levels of histone phosphorylation. IL-1β induces neuronal hyperexcitability and is released under conditions of psychological stress and fever; both known triggers of clinical HSV reactivation. IL-1β treatment of sympathetic neurons induced histone phosphorylation, and importantly HSV reactivation, which was dependent on both DLK and neuronal excitability. Thus, HSV co-opts an innate immune pathway resulting from IL-1 stimulation of sympathetic neurons to induce reactivation from latency.

Introduction

Herpes simplex virus-1 (HSV-1) is a ubiquitous human pathogen that is present in approximately 40-90% of the population worldwide[1]. HSV-1 persists for life in the form of a latent infection in neurons, with intermittent episodes of reactivation. Reactivation from a latent infection and subsequent replication of the virus can cause substantial disease including oral and genital ulcers, herpes keratitis and encephalitis. In addition, multiple studies have linked persistent HSV-1 infection to the progression of Alzheimer's disease[2]. Stimuli in humans that are linked with clinical HSV-1 reactivation include exposure to UV light, psychological stress, fever and changes in hormone levels[3]. How these triggers result in reactivation of latent HSV-1 infection is not fully understood.

During a latent infection of neurons, there is evidence that the viral genome is assembled into a nucleosomal structure by associating with cellular histone proteins[4]. The viral lytic promoters have modifications that are characteristic of silent heterochromatin (histone H3 di- and tri-methyl lysine 9; H3K9me2/3, and H3K27me3)[5-8], which is thought to maintain long-term silencing of the viral lytic transcripts. Hence, for reactivation to occur, viral lytic gene expression is induced from promoters that are assembled into heterochromatin and in the absence of viral proteins, such as VP16, which are important for lytic gene expression upon *de novo* infection. Reactivation is therefore dependent on the host proteins and the activation of cellular signaling pathways[3]. However, the full nature of the stimuli that can act on neurons to trigger

66 reactivation and the mechanisms by which expression of the lytic genes occurs have
67 not been elucidated.
68
69 One of the best characterized stimuli of HSV reactivation at the cellular level is
70 nerve-growth factor (NGF) deprivation resulting from loss of PI3K/AKT activity[9-11].
71 Previously, we found that activation of activation of the c-Jun N-terminal kinase (JNK)
72 cell stress response via activation of dual leucine zipper kinase (DLK) was required for
73 reactivation in response to loss of NGF signaling. In addition, recent work has identified
74 a role for JNK in HSV reactivation following perturbation of the DNA damage/repair
75 pathways, which also trigger reactivation via inhibition of AKT activity[12]. DLK is a master
76 regulator of the neuronal stress response, and its activation can result in cell death,
77 axon pruning, axon regeneration or axon degeneration depending on the nature of
78 activating trigger[13,14]. Therefore, it appears that HSV has coopted this neuronal stress
79 pathway of JNK activation by DLK to induce reactivation. One key mechanism by which
80 JNK functions to promote lytic gene expression is via a histone phosphorylation on S10
81 of histone H3[15]. JNK-dependent histone phosphorylation occurs on histone H3 that
82 maintains K9 methylation and is therefore known as a histone methyl/phospho switch,
83 which permits transcription without the requirement for recruitment of histone
84 demethylases[16,17]. This initial wave of viral lytic gene expression is known as Phase I,
85 and also occurs independently of the lytic transactivator VP16. In addition, late gene
86 expression in Phase I occurs independent of viral genome replication[18,19]. A sub-
87 population of neurons then progress to full reactivation (also known as Phase II), which
88 occurs 48-72h post-stimulus and requires both VP16 and histone demethylase activity

[15,20-23]. However, not all models of reactivation appear to go through this bi-phasic progression to reactivation as axotomy results in more rapid viral gene expression and dependence on histone demethylase activity for immediate viral gene expression.

The aim of this study was to determine if we could identify novel triggers of HSV reactivation and determine if they involved a bi-phasic mode of reactivation. We decided to focus on stimuli that cause heightened neuronal activity because hyperstimulation of cortical neurons following forskolin treatment or potassium chloride mediated depolarization has previously been found to result in a global histone methyl/phospho switch[24]. Whether this same occurs in different types of neurons, including sympathetic neurons, is not known. Although forskolin has previously been found to induce HSV reactivation,[25-28], whether this is a result of inducing hyperexcitability or as a consequence of activation of alterative cAMP-responsive proteins including PKA and CREB is not known. Therefore, we investigated if forskolin-mediated reactivation was a result of increased neuronal activity. Hyperexcitability of neurons is correlated with changes in cellular gene expression, increased DNA damage[29,30] and epigenetic changes including H3 phosphorylation[24]. However, DLK-mediated activation of JNK has not been linked to changes in cellular gene expression in response to hyperexcitability. Therefore, we were also interested in determining whether DLK and JNK are required for induction of HSV gene expression in response to hyperexcitability.

IL-1β is released under conditions of psychological stress and fever[31-34]; both known triggers of clinical HSV reactivation[35-37]. IL-1β has previously been found to

induce heightened neuronal activity[38-40]. However, an intriguing feature of IL-1β signaling is its ability to have differential effects on different cell types. For example, IL-1β is involved extrinsic immune response to infection via activation of neutrophils and lymphocytes. In addition, it can act on non-immune cells including fibroblasts to initiate an antiviral response[41,42], as has previously been described for lytic infection with HSV-1[41]. Given these differential downstream responses to IL-1β signaling, we were particularly interested in the effects of IL-1β treatment of latently infected neurons. Interestingly, we found that IL-1β was capable of inducing reactivation of HSV from mature sympathetic neurons. Inhibition of voltage-gated sodium and hyperpolarization activated cyclic nucleotide gated (HCN) channels prevented reactivation mediated by both forskolin and IL-1β. Activity of the cell stress protein DLK was also essential for IL-1β-mediated reactivation. We therefore identify IL-1β as a novel trigger from HSV reactivation that acts via neuronal hyperexcitability and highlight the central role of JNK activation by DLK in HSV reactivation.

Results

Adenylate Cyclase Activation Triggers DLK/JNK-Dependent Reactivation of HSV from Latent Infection in Sympathetic Neurons

Both forskolin and cAMP mimetics are well known to induce neuronal hyperexcitation and have previously also been found to trigger HSV reactivation[25-28]. Using a model of HSV latency in mouse sympathetic neurons isolated from the super-cervical ganglia (SCG)[15] we investigated whether forskolin treatment induced reactivation in this system and the potential mechanism resulting in the initial induction

of viral lytic gene expression. Sympathetic SCG neurons were infected with a Us11-GFP tagged HSV-1[43] at a multiplicity of infection (MOI) of 7.5 PFU/cell in the presence of acyclovir (ACV). After 6 days the ACV was washed out and the neuronal cultures monitored to ensure that no GFP-positive neurons were present. Two days later, reactivation was triggered by addition of forskolin (Figure 1A). As represented in figure 1B, forskolin can act either extra-cellularly on ion channels or intracellularly to activate adenylate cyclase[44-46]. Dideoxy-forskolin is a cell impermeable forskolin analog that can act directly on voltage gated ion channels but does not activate cAMP[44,47]. We found addition of forskolin but not dideoxy-forskolin triggered HSV reactivation (Figure 1C). In addition, treatment of latently infected primary neurons with a cAMP mimetic (8-bromo-cAMP) was sufficient to trigger reactivation (Figure 1D) and inhibition of adenylate cyclase activity using SQ22, 536[48] significantly diminished HSV reactivation (Figure 1E). Therefore, activation of adenylate cyclase activation and subsequent increased intracellular levels of cAMP are required for forskolin-mediated reactivation.

DLK/JNK Activity is Required for the Early Phase of Viral Gene Expression in Response to Forskolin Treatment

We previously found that DLK-mediated JNK activation was essential for Phase I reactivation following interruption of nerve growth factor signaling. To determine whether DLK and JNK activation were crucial for reactivation in response to hyperexcitability, neurons were reactivated with forskolin in the presence of the JNK-inhibitor SP600125 (Fig. 2A) or the DLK inhibitor GNE-3511[49] (Fig. 2B), which prevented reactivation based on the number of GFP-positive neurons at 3-days post-

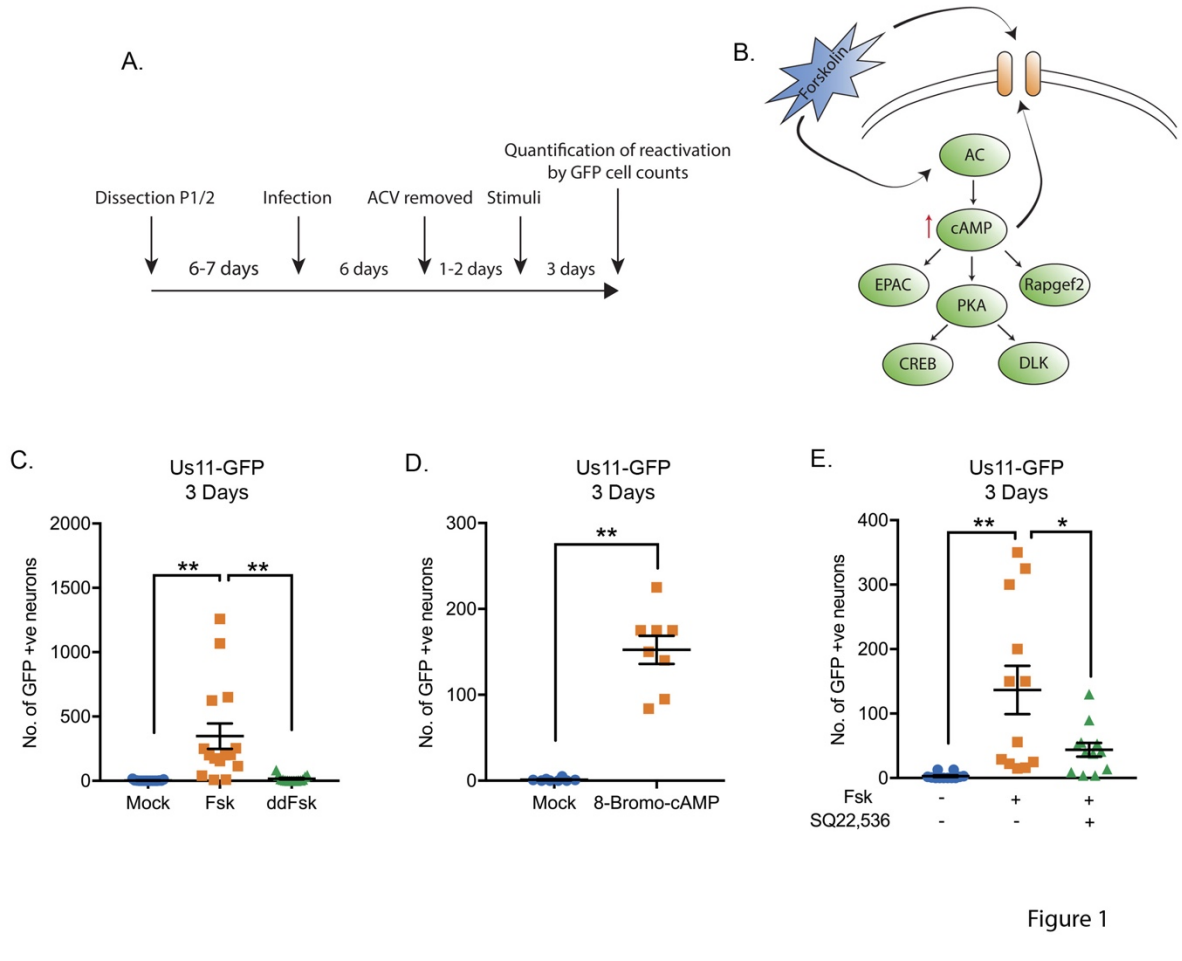

Figure 1

Figure 1. HSV-1 Reactivation Induced by Adenylate Cyclase Activation is DLK/JNK-Dependent. (A) Schematic of the primary superior sympathetic ganglia-derived model of HSV latency. Reactivation was quantified based on Us11-GFP positive neurons in presence of WAY-150168, which prevents cell-to-cell spread. (B) Schematic of the cellular pathways activated by forskolin treatment. Forskolin can act both intracellularly to activate adenylate cyclase increasing the levels of cAMP or extracellularly on ion channels. (C) HSV reactivation was induced by treatment with forskolin (60μM) but not the cell-impermeable dideoxy-forskolin (60μM). (D) Reactivation could be triggered by the cAMP mimetic 8-Bromo-cAMP (125μM). (E) Forskolin-induced reactivation was blocked by the adenylate cyclase inhibitor SQ22,536 (50μM). Each point represents a single replicate. Statistical comparisons were made using Welch's t-test.

158 reactivation Inhibition of either JNK or DLK blocked HSV reactivation in response to
159 forskolin. These data therefore indicate hyperexcitability-induced reactivation is
160 dependent on the neuronal stress pathway mediated by DLK activation of JNK.
161
162 Because we previously found that JNK-activation results in a unique wave of viral
163 gene expression in response to inhibition of nerve-growth factor signaling, we especially
164 intrigued to determine whether hyperexcitability triggers a similar wave of JNK
165 dependent viral gene expression. The previously described bi-phasic progression to
166 viral reactivation is characterized by viral DNA replication and production of infectious
167 virus, occurring around 48-72 post-stimulus[18], but an earlier wave of lytic gene
168 expression occurring around 20h post-stimulus. To determine whether forskolin-
169 mediated reactivation results in a similar kinetics of reactivation, we investigated the
170 timing of Us11-GFP synthesis, viral DNA replication, production of infectious virus and
171 lytic gene induction following forskolin treatment. In response to forskolin treatment,
172 GFP synthesis in neurons started to appear around 48h post-reactivation, with more
173 robust reactivation observed at 72h (Figure 2C). In contrast to forskolin-mediated
174 reactivation, the number of GFP-positive neurons following superinfection with a
175 replication competent wild-type virus resulted in a rapid induction of GFP-positive
176 neurons by 24h post-superinfection (Figure 2C). Therefore, forskolin triggered
177 reactivation results in slower synthesis of Us11-GFP than superinfection. In addition,
178 these data highlight the ability of forskolin to trigger reactivation from only a
179 subpopulation of latently infected neurons (approximately 1 in every 3.4 neurons
180 compared to superinfection).

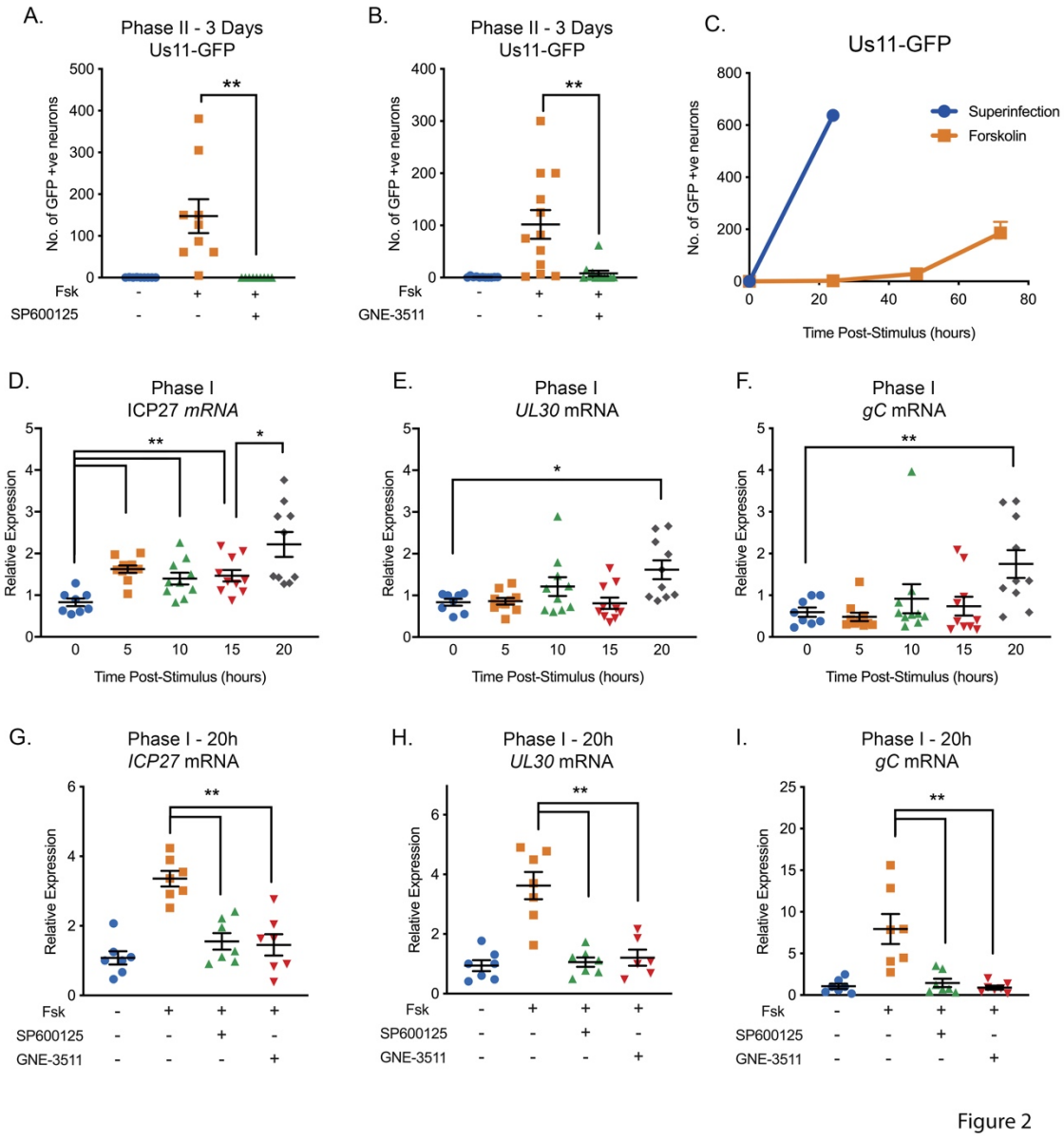

Figure 2. Reactivation Triggered by Forskolin Involves a DLK/JNK Dependent Phase I of Viral Gene Expression.

(A) Reactivation was induced by forskolin in the presence of JNK inhibitor SP600125 (20μM). (B) Reactivation was induced by forskolin in the presence of the DLK inhibitor GNE-3511 (4μM). (C) Reactivation was induced by forskolin or superinfection with a wild-type (F strain) HSV-1 (MOI of 10 PFU/cell) and qualified based on Us11-GFP positive neurons (n=3). (D-F) RT-qPCR for viral mRNA transcripts following forskolin treatment of latently infected SCGs. (G-I) RT-qPCR for viral lytic transcripts at 20h post-forskolin treatment and then in presence of the JNK inhibitor SP600125 (20μM) and the DLK inhibitor GNE-3511 (4μM). In D-L each experimental replication is represented. Statistical comparisons were made using two-tailed paired student's t-test.

181

182

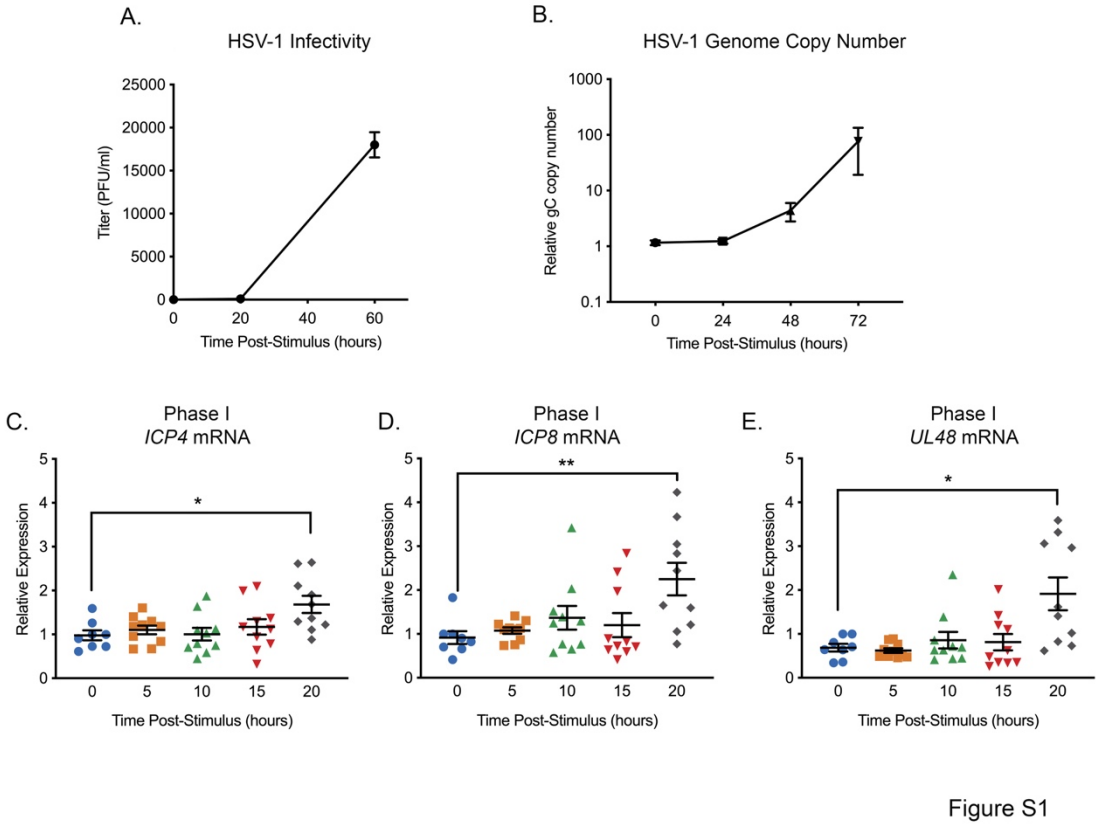

Figure S1

Figure S1(A) Reactivation triggered by forskolin triggers a wave of lytic gene expression that precedes DNA replication and infectious virus production (supplement to Figure 2)
(A) Titers of infection virus detected from reactivating neurons induced with forskolin (n=4). (B) Quantification of the relative viral genome copy number following forskolin-mediated reactivation based on gC copy number normalized to cellular GAPDH and expressed relative to the 0h time-point (n=7). (C-E) RT-qPCR for viral mRNA transcripts following forskolin treatment of latently infected SCGs. In C-E each biological replicate is represented. Statistical comparisons were made using two-tailed paired student's t-test (C-E).

183

184

The production of infectious virus also mirrored the data for the detection of Us11-GFP positive neurons, with a robust increase in viral titers between 24 and 60h post-stimulus (Figure S1A). An increase in viral genome copy was also not detected until 48h post-stimulus, which continued between 48h and 72h (Figure S1B). The quantification of viral genome copy number was also carried out in presence of WAY-150138[50], which prevents packaging of the viral genome[51], therefore indicating that DNA replication occurs in reactivating neurons and not as a consequence of cell-to-cell spread.

Given the observed 48h delay in viral DNA replication and production of infectious virus, we were interested to determine if there was a Phase I wave of lytic gene expression that occurred prior to viral DNA replication. We therefore carried out RT-qPCR to detect representative immediate-early (*ICP27* and *ICP4*), early (*ICP8* and *UL30*) and late (*UL48* and *gC*) transcripts between 5- and 20-hours post addition of forskolin (Figures 2D-F and S1C-E). For all six transcripts, a significant up-regulation of mRNA occurred at 20h post-treatment, including the true late gene *gC*, whose expression would usually only be stimulated following viral genome replication in the context of *de novo* lytic replication. Therefore, this indicates that lytic gene expression is induced prior to viral DNA replication and that neuronal hyperexcitability does trigger a Phase I wave of lytic gene expression. Notably, we did detect small but reproducible induction of *ICP27* mRNA at 5h post-stimulus, followed by a second induction at 20h (Figure 2D), indicating that there is likely differential regulation of some viral lytic

transcripts during Phase I reactivation induced by hyperexcitability that is distinct from both NGF-deprivation and *de novo* lytic infection.

To determine whether JNK and DLK were required Phase I gene expression in response to hyperexcitability, we investigated viral mRNA levels following forskolin-mediated reactivation in the presence of the JNK inhibitor SP600125. We found a significant reduction in *ICP27* (2.2-fold), *UL30* (3.3-fold) and *gC* (5.5-fold) mRNA levels at 20h post-stimulus in the presence of SP600125 (Figure 2J-L). For all genes tested, there was no significant increase in mRNAs in the JNK-inhibitor treated neurons compared to mock. We observed comparable results following treatment with the DLK inhibitor GNE-3511, with a 2.3-, 3-, 8.8-fold decrease in *ICP27*, *UL30* and *gC* mRNAs respectively compared to forskolin treatment alone, and no significant increase in mRNA levels compared to the reactivated samples (Figure 2J-L).

It is possible that in addition to JNK, other signal transduction proteins are important in forskolin-mediated reactivation. Previous data has found that DLK can be activated by PKA, which is well known to be activated by cAMP. However, using well characterized inhibitors of PKA, along with the PKA-activated transcription factors CREB, in addition to two other cAMP responsive proteins Rapgef2 and EPAC, we did not find that these cAMP activated proteins were required for Phase I reactivation (Figure S2). Inhibition of PKA or CREB did reduce Phase II reactivation (Figure S2A and C) but had no effect on Phase I (Figure S2B and D). Inhibition of Rapgef2 or PEAC had no effect on HSV reactivation (Figure SE and F). Taken together, these data

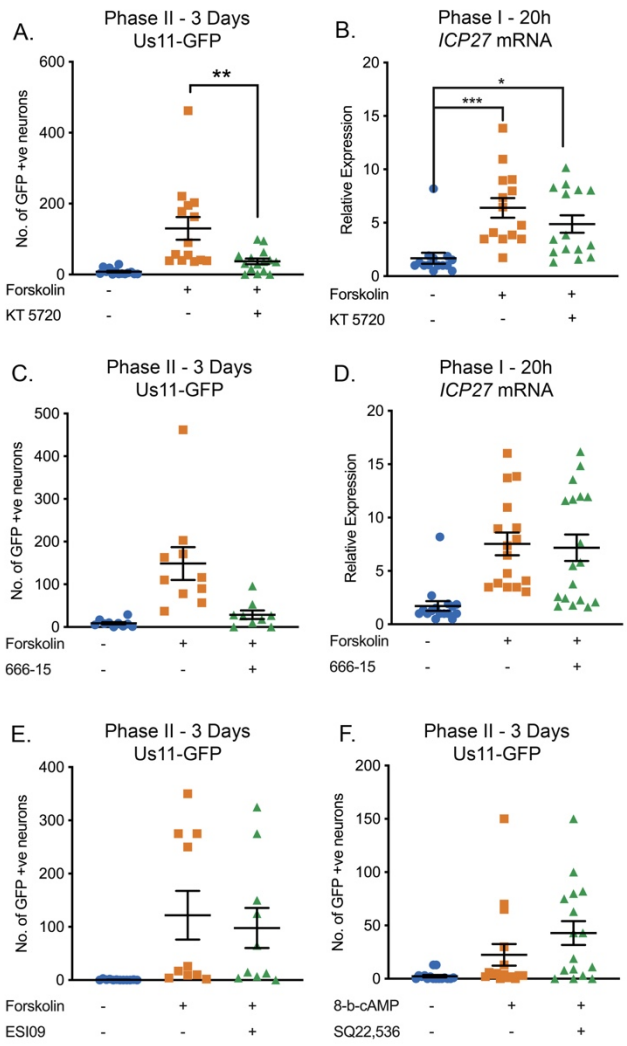

Figure S2

Figure S2. Effect of PKA, CREB, Rapgef2 and EPAC Inhibition on HSV-1 Reactivation. (A) Latently infected cultures were reactivated with forskolin (60 μM) in the presence of the PKA inhibitor KT 5720 (3 μM) and the number of Us11-GFP positive neurons quantified at 3 days post-reactivation. (B) RT-qPCR for the viral lytic transcript ICP27 at 20h post-forskolin treatment and in the presence of KT 5720. (C) Latently infected cultures were reactivated with forskolin in the presence of the CREB inhibitor 666-15 (2 μM). (D) RT-qPCR for ICP27 at 20h post-forskolin treatment and in the presence of 666-15. (E) Latently infected cultures were reactivated with forskolin (60μM) in the presence of the EPAC inhibitor ESI09 (10 μM). (F) Latently infected cultures were reactivated with 8-Bromo-cAMP (125μM) in the presence of the Rapgef2 inhibitor SQ22,536 (50 μM). Individual experimental replicates are represented. Statistical comparisons were made using Welch's t-test (A) or two-tailed unpaired t-test (B).

230

231

232 indicate that it is hyperexcitability induced by forskolin that induces a Phase I wave of
233 gene expression via activation of DLK and JNK.
234
235 Forskolin Triggers a Phase-I Wave of Viral Gene Expression that is Independent of
236 Histone Demethylase Activity.
237 Hyperexcitability results in the propensity of neurons to fire repeated action
238 potentials, and is associated with specific changes in histone posttranslational
239 modifications. The first is physiological DNA damage[29,30], measured by the intensity of
240 γH2AX staining in neuronal nuclei. Forskolin treatment was associated with an increase
241 in the levels of γH2AX at 5h post-treatment, which resolved by 15h post-treatment
242 (Figure S2A and C), and is therefore indicative of physiological DNA damage and
243 repair, which occurs upon neuronal hyperexcitability. A second reason for probing the
244 DNA damage/repair pathway in response to forskolin treatment is that previously
245 reactivation of HSV from latency has been associated with perturbation of the DNA
246 damage/repair response[12]. Both inhibition of repair and exogenous DNA damage
247 resulted in loss of AKT phosphorylation by PHLPP1, which was required for HSV
248 reactivation. Although we did observe increased levels of γH2AX following forskolin
249 treatment, this was not accompanied by a loss of pAKT measured at 15h post-treatment
250 (Figure S2D). This indicates that HSV reactivation in response to forskolin treatment
251 does not involve dephosphorylation of AKT. Therefore, hyperexcitability triggers
252 reactivation via an alternative mechanism that does not feed into the AKT.
253

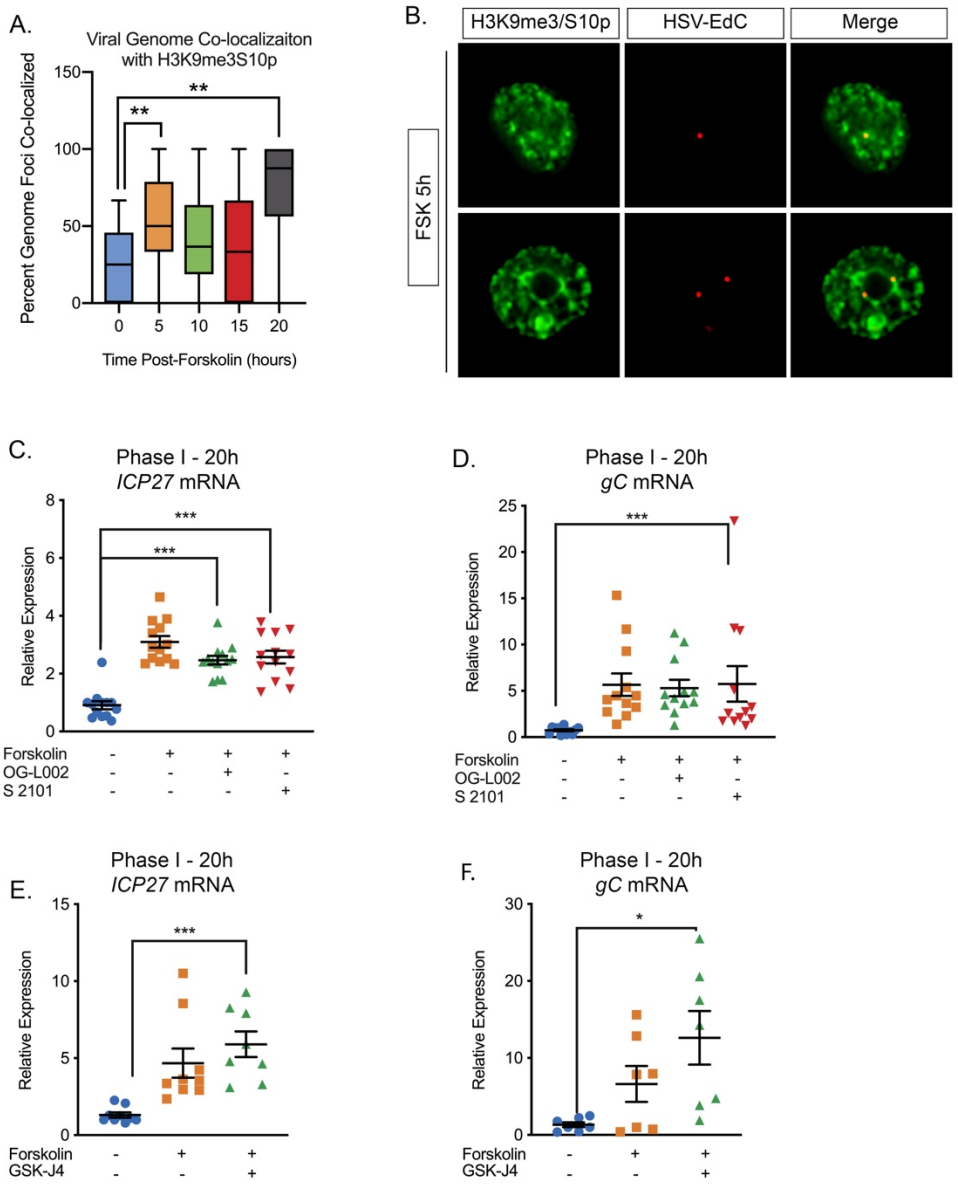

Figure 3

Figure 3. The Initial Wave of Viral Lytic Gene Expression During Forskolin-mediated Reactivation is Independent on Histone Demethylase Activity. (A) Quantification of the percentage of genome foci stained using click-chemistry that co-localize with H3K9me3/S10p. At least 15 fields of view were blindly scored from two independent experiments. Whiskers represent the 2.5-97.5 percentile range. (B) Representative images of click-chemistry based staining of HSV-EdC genomes and H3K9me3/S10p staining at 5h post-forskolin treatment. (C and D). Effect of the LSD1 inhibitors OG-L002 and S 2101 on forskolin-mediated Phase I of reactivation determined by RT-qPCR for ICP27 (C) and gC (D) viral lytic transcripts at 20h post-forskolin treatment and in the presence of 15μM OG-L002 and 20μM S 2102. (E) Effect of the JMJD3 and UTX inhibitor GSK-J4 (2μM) on forskolin-mediated Phase I measured by RT-qPCR for viral lytic transcripts ICP27 (E) and gC (F) at 20h post-forskolin treatment and in the presence of GSK-J4. For C-F each experimental replicate is represented. Statistical comparisons were made using two-tailed unpaired t-test (A) or Welch's t-test (C-F).

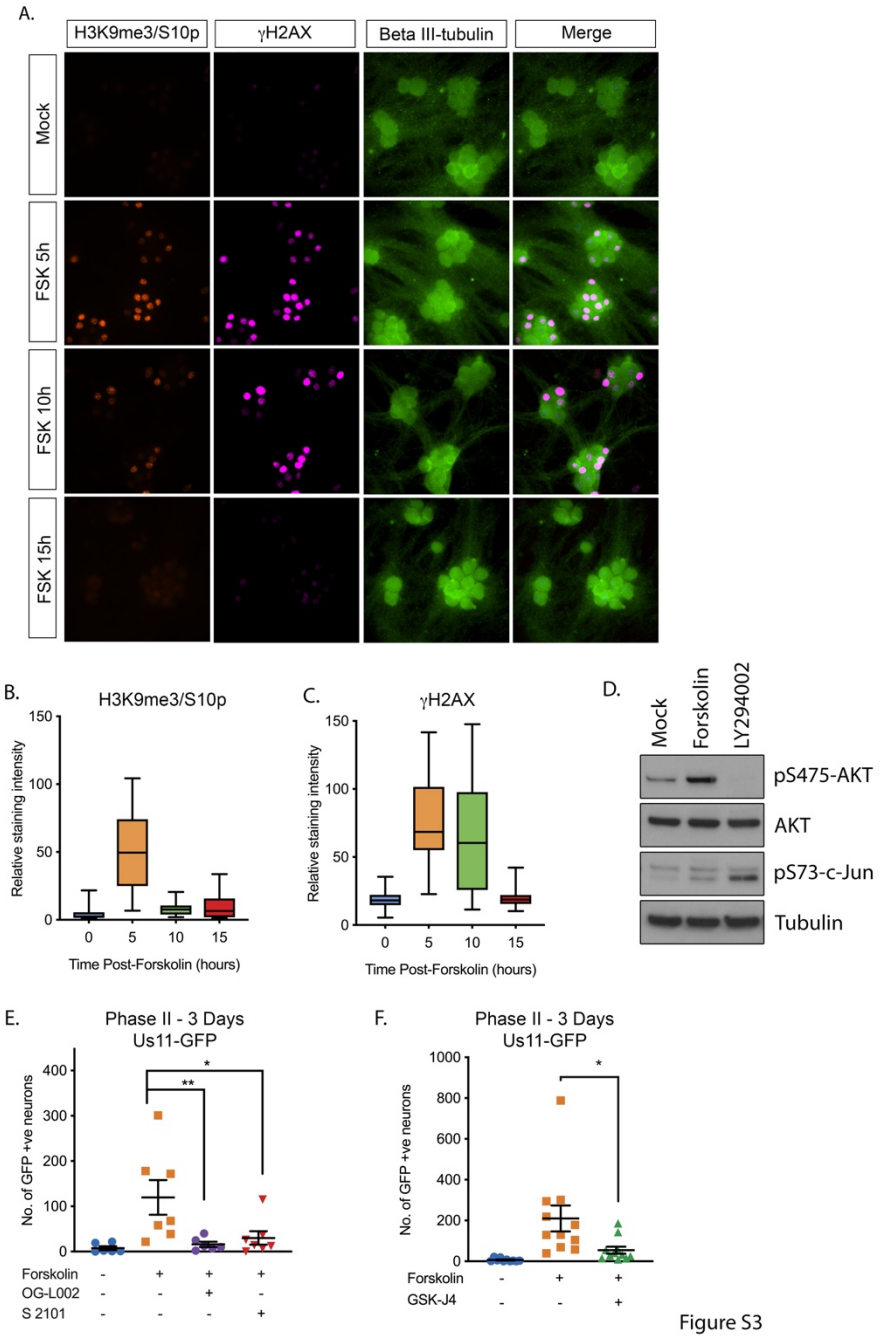

Figure S3

Figure S3. Forskolin Treatment Induces Hyperexcitability-associated Histone Post-translational Modification in Sympathetic Neurons. SCG neurons were treated with forskolin and immunofluorescence staining was carried out for H3K9me3/S10p, the DNA damage marker γH2AX and the neuronal marker beta III-tubulin. (B) Quantification of neuronal nuclear staining intensity for H3K9me3 (>150 cells/condition). (C) Quantification of neuronal nuclear staining for γH2AX. In B and C, whiskers represent the 2.5-97.5 percentile range. (D). Western blotting for pS475-AKT, total AKT, pS73-c-Jun and tubulin at 15h post-treatment with the PI3-kinase inhibitor LY294002 (20μM) or forskolin (60 μM). (E) Effect of the LSD1 inhibitors OG-L002 (15μM) and S 2101 (20μM) on forskolin-mediated reactivation measured by Us11-GFP positive neurons. (F) Effect of the JMJD3

and UTX inhibitor GSK-J4 (2μM) on forskolin-mediated reactivation measured by Us11-GFP positive neurons. Statistical comparisons were made using Welch's t-test (E, F).

Previously, we found that Phase I reactivation is accompanied with a JNK-dependent histone methyl/phospho (marked by H3K9me3/pS10) switch on lytic promoters[15]. In cortical neurons, one study has found that hyperexcitability results in increased H3K9me3/pS10[24]. Therefore, we were particularly interested to determine whether forskolin treatment of sympathetic neurons triggered a histone S10 phosphorylation on H3K9me3. Forskolin triggered a transient increase in H3K9me3/S10p at 5h post-treatment that had returned to baseline by 10h (Figure S3A and B). This indicates that, in keeping with cortical neurons, forskolin induces a histone H3K9me3/pS10 methyl/phospho switch on regions on cellular chromatin.

We next sought to determine whether the phospho/methyl switch that arises as a result of hyperexcitability plays a role in Phase I of HSV reactivation. We therefore investigated whether viral genomes were co-localized with H3K9me3/S10p following forskolin treatment. To visualize HSV genomes, viral stocks were grown in the presence of EdC as described previously[52,53]. Click-chemistry was performed on latently infected and neurons following forskolin treatment. As shown in Figure 3A and B, viral genomes co-localized with H3K9me3/pS10 following robust H3K9me3/S10p staining at 5h. The percentage of viral genomes that co-localized with H3K9me3/S10p was significantly increased compared to the unreactivated samples at 5h and 20h post-forskolin treatment (Figure 3A).

Serine phosphorylation adjacent to a repressive lysine modification is thought to permit transcription without the removal of the methyl group[17,24]. Therefore, we investigated whether histone demethylase activity was required for the initial induction in lytic gene expression following forskolin treatment. Previously, the H3K9me2 histone demethylase LSD1 has been found to be required for full HSV reactivation[20,23], and in our in vitro model this was determined by the production of infectious viral particles or late gene synthesis at 48-72h post-reactivation[15]. Addition of two independent LSD1 inhibitors (OG-L002 and S 2102) inhibited Us11-GFP synthesis at 72h post-reactivation (Figure 3C). Hence, LSD1 activity, and presumably removal of H3K9-methylation is required for forskolin-mediated reactivation. However, LSD1 inhibition did not prevent the initial induction of *ICP27* and *g*C mRNA expression at 20h post-forskolin treatment (Figure 3D and E). Therefore, this initial wave of viral lytic gene expression following forskolin-mediated reactivation is independent of histone H3K9 demethylase activity.

We previously found that H3K27me demethylase activity is required for full reactivation but not the initial wave of gene expression[15]. However, because of the lack of an antibody that specifically recognizes H3K27me3S28p and not also H3K9me3S10p, we are unable at this point to investigate genome co-localization with this combination of modifications. However, we could investigate the role of the H3K27me demethylases in forskolin-mediated reactivation. Treatment of neurons with the UTX/JMJD3 inhibitor GSK-J4[54] prevented the synthesis of Us11-GFP at 72h post-reactivation, indicating that removal of K27 methylation is required full reactivation (Figure 3F). However, the initial burst of gene expression (assessed by *ICP27* and *gC*

mRNA levels) was robustly induced at 20h post-forskolin treatment in the presence of GSK-J4 (Figure 3G and H). Taken together, our data indicate that the initial phase of gene expression following forskolin treatment is independent of histone demethylase activity and therefore consistent with a role for a histone methyl/phospho switch in permitting lytic gene expression.

Forskolin-Mediated Reactivation Requires Neuronal Excitability

Given that the HSV genome co-localized with regions of hyperexcitability-induced changes in histone phosphorylation, we investigated whether reactivation was linked to neuronal excitability. To inhibit action potential firing, we treated neurons with tetrodotoxin (TTX), which inhibits the majority of the voltage gated sodium channels and therefore depolarization. Addition of TTX significantly inhibited HSV reactivation triggered by forskolin, as measured by Us11-GFP positive neurons at 72 hours post-stimulus (Figure 4A). To further confirm a role for repeated action potential firing in forskolin-mediated reactivation, we investigated the role of voltage gated potassium channels, which are required for membrane repolarization. Addition of TEA, which inhibits voltage-gated potassium channel activity, also blocked HSV reactivation measure by Us11-GFP positive neurons at 3 days post-forskolin treatment (Figure S4B. Taken together, these data indicate that action potential firing is required for forskolin-mediated reactivation.

Increased levels of cAMP can act on nucleotide gated ion channels, including the hyperpolarization activated cyclic nucleotide gated (HCN) channels. HCN channels are

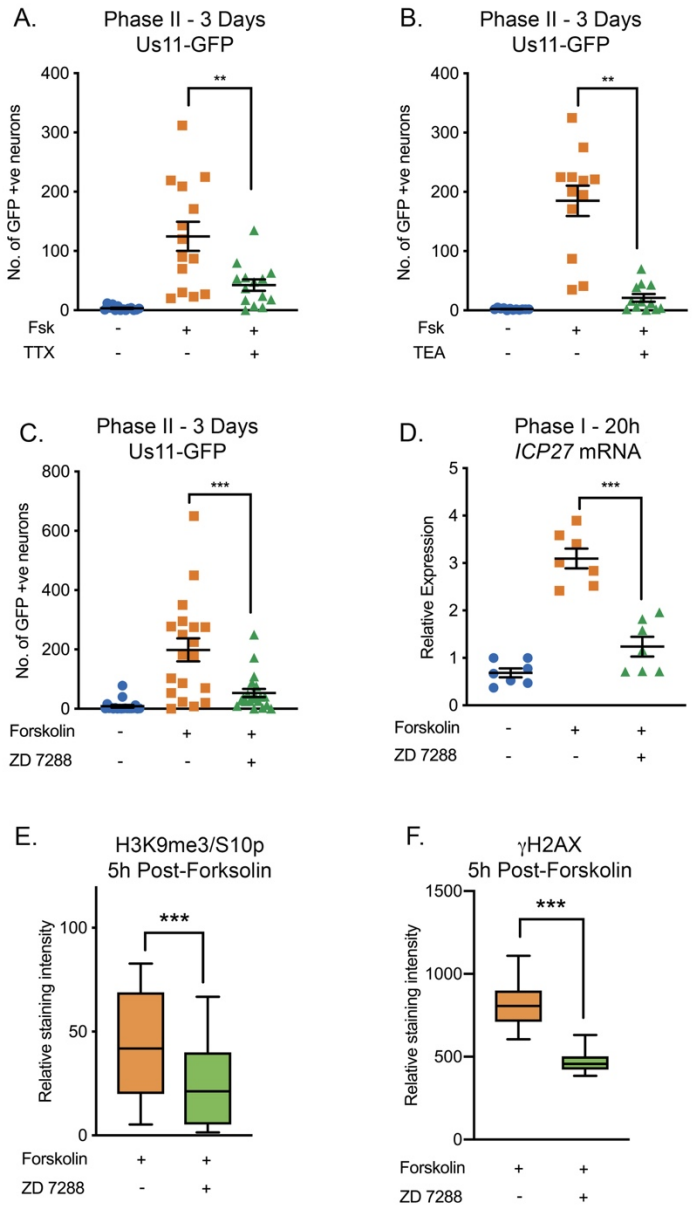

Figure 4

Figure 4. HSV Reactivation Mediated by Forskolin Requires Neuronal Activity.
(A) Latently infected cultures were reactivated with forskolin in the presence of the voltage-gated sodium channel blocker tetrodotoxin (TTX; 1μM) and the number of Us11-GFP positive neurons quantified at 3 days post-reactivation. (B) Latently infected cultures were reactivated with forskolin in the presence of the voltage-gated potassium channel blocker Tetraethylammonium (TEA; 10 mM) and the number of Us11-GFP positive neurons quantified at 3 days post-reactivation. (C) Forskolin-mediated reactivation in the presence of the HCN channel blockers ZD 7288 (10μM) quantified as the numbers of Us11-GFP positive neurons at 3 days post-reactivation. (D) The effect of ZD 7288 on the HSV lytic gene transcript ICP27 during Phase I reactivation measured at 20h post-forskolin treatment by RT-qPCR. Individual experimental

replicates are represented. (E and F) Quantification of the relative nuclear staining for H3K9me3/S10p and γH2AX in SCG neurons at 5h post-forskolin treatment and in the presence of ZD 7288 from two independent experiments. Statistical comparisons were made using Welch's t-test (A-C), two-tailed unpaired t-test (D-F).

K^+ and Na^+ channels that are activated by membrane hyperpolarization[55,56]. In the presence of high levels of cAMP, the gating potential of HCN channels is shifted in the positive direction, such that HCN channels can open at resting membrane potential, resulting in an increased propensity of neurons to undergo repeated firing[56-58]. HCN channel activity can be blocked by ZD 7288, Ivabradine or cesium chloride. Addition of ZD 7288 (Figure 4A), Ivabradine (Figure S4A) or CsCl (Figure S4B) all significantly reduced HSV reactivation triggered by forskolin, as measured by Us-11 GFP positive neurons at 3 days post-stimulus. To determine whether HCN channel activity was required for the initial induction of HSV lytic mRNA expression, we assessed viral mRNA expression during Phase I in the presence and absence of ZD 7288. Expression of representative lytic mRNAs *ICP27* (Figure 4D), *UL30* and *gC* (Figure S4C and D) were significantly decreased in the presence of ZD 7288 compared to the forskolin treated neurons alone, and were not significantly increased compared to the mock treated samples. Therefore, HCN channel activity is required for the initial induction of lytic gene expression during Phase I reactivation mediated by forskolin.

We also confirmed that inhibition of HCN-channel activity affected the levels of hyperexcitability-associated changes in histone post-translational modifications. Addition of ZD 7288 resulted in significantly decreased staining intensities of both H3K9me3/S10p and γH2AX at 5h post-forskolin treatment (Figure 4F and G), which was the peak time-point for which we observed these changes upon forskolin treatment alone (Figure S3 A and B). Therefore, activity of the HCN channels in response to

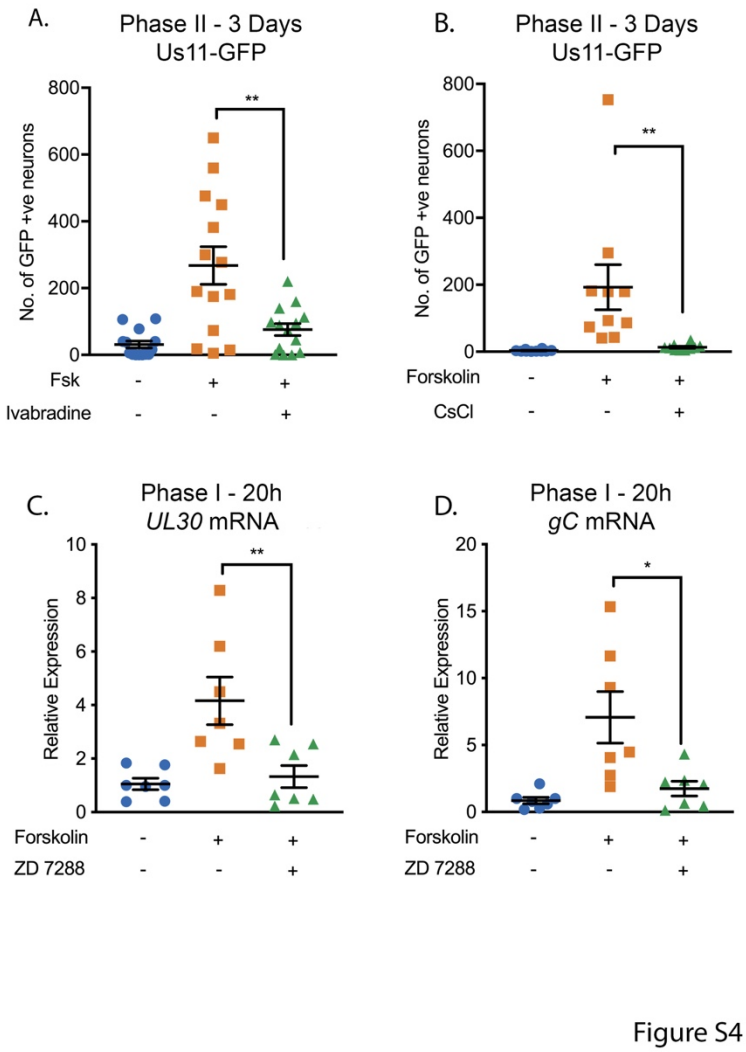

Figure S4

Figure S4. HSV Reactivation Mediated by Forskolin Requires Neuronal Activity. (A and B) Latently infected cultures were reactivated with forskolin in the presence of the HCN channel inhibitors ivabradine (20μM; A) and CsCl (3mM; B). Latently infected cultures were reactivated with forskolin in the presence of the HCN inhibitor ZD 7288 (10 μM) and viral lytic transcripts measured at 20h post-reactivation. Individual experimental replicates are represented. Statistical comparisons were made using Welch's t-test (A, B) or two-tailed unpaired t-test (C, D).

344

345

346 increased levels of cAMP results in hyperexcitability-associated changes in
347 histone modifications and reactivation of HSV from latent infection.
348
349 HSV Reactivation can be Induced by Stimuli that Directly Increase Neuronal Excitability
350 The role of ion-channel activity in forskolin-mediated reactivation prompted us to
351 investigate whether additional stimuli that induce hyperexcitability in neurons also
352 trigger HSV reactivation. We were also interested in whether reactivation required
353 chronic versus short term hyperexcitability. Increasing the extracellular concentration of
354 KCl is well-known to induce action potential firing. Therefore, we investigate the timing
355 of both KCl and forskolin-mediated hyperexcitability in HSV reactivation. Both of these
356 treatments triggered HSV reactivation more robustly if applied for 8h or more (Figure
357 5A). This indicates that chronic neuronal hyperactivity is important in inducing
358 reactivation of HSV.
359
360 To further clarify that hyperexcitability can directly trigger HSV reactivation, we
361 investigated the effects of removal from a TTX block on latently infected neurons.
362 Addition of TTX to neurons results in synaptic scaling, so that when the TTX is removed
363 the neurons enter a hyperexcitable state[59-62]. TTX was added to the neurons for 2 days
364 and then washed out. This resulted in a robust HSV reactivation as determined by
365 Us11-GFP synthesis (Figure 5B). We also investigated whether the JNK-cell stress
366 pathway was important in HSV reactivation in response to TTX-release. Addition of the
367 JNK inhibitor SP600125 or the DLK inhibitor, GNE-3511, blocked HSV reactivation

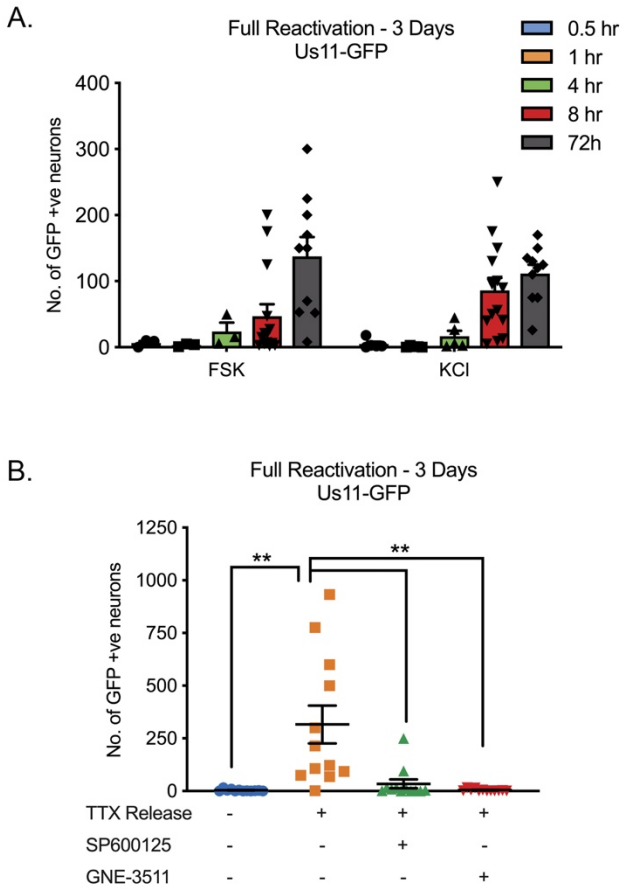

Figure 5

Figure 5. HSV Reactivation Triggered by Prolonged Neuronal Hyperexcitability is DLK/JNK Dependent. (A) Latently infected SCG cultures were treated with forskolin or KCl (55mM) for the indicated times followed by wash-out. Reactivation was quantified by number of Us11-GFP positive neurons at 3 days after the initial stimulus was added. (B) Latently infected neurons were placed in tetrodotoxin (TTX; 1μM) for 2 days and the TTX was then washed out. At the time of wash-out the JNK inhibitor SP600125 (20μM) or DLK inhibitor GNE-3511 (4μM) was added. Reactivation was quantified at 3-days post-wash-out. Individual experimental replicates are represented. Statistical comparisons were made using Welch's t-test.

following TTX-release. Therefore, directly inducing neuronal hyperexcitability triggers HSV reactivation in a DLK/JNK-dependent manner.

IL-1β Triggers HSV Reactivation in Mature Neurons in a DLK and HCN Channel Dependent Manner

Our data thus far point to a reactivation of HSV following increasing episodes of neuronal hyperexcitability in a way that is requires activation of the JNK-cell stress pathway. However, we wished to link this response to a physiological trigger that may stimulate HSV reactivation *in vivo*. Increased HCN-channel activity has been associated to inflammatory pain resulting from the activity of pyrogenic cytokines on neurons[63]. In addition, IL-1β is known to act on certain neurons to induce neuronal excitation[38-40]. IL-1β is released in the body during times of chronic, psychological stress. In addition, IL-1β contributes to the fever response[31-34]. In sympathetic neurons, we found that exposure of mature neurons to IL-1β induced an accumulation of the hyperexcitability-associated histone post-translational modifications γH2AX and H3K9me3/S10p (Figure 6A-C). We did not observe the same changes for post-natal neurons. The reasons for this maturation-dependent phenotype are unknown at this point but we hypothesize it could be due to changes in the expression of cellular factors required to respond to IL-1β. Therefore, these experiments were carried out on neurons that we more than 28 days old. The kinetics of induction of these histone modifications was different from what we had previously observed for forskolin treatment, as both γH2AX and H3K9me3/S10p steadily accumulated to 20h post-treatment. This likely reflects the activation of upstream signaling pathways in response to IL-1β prior to inducing

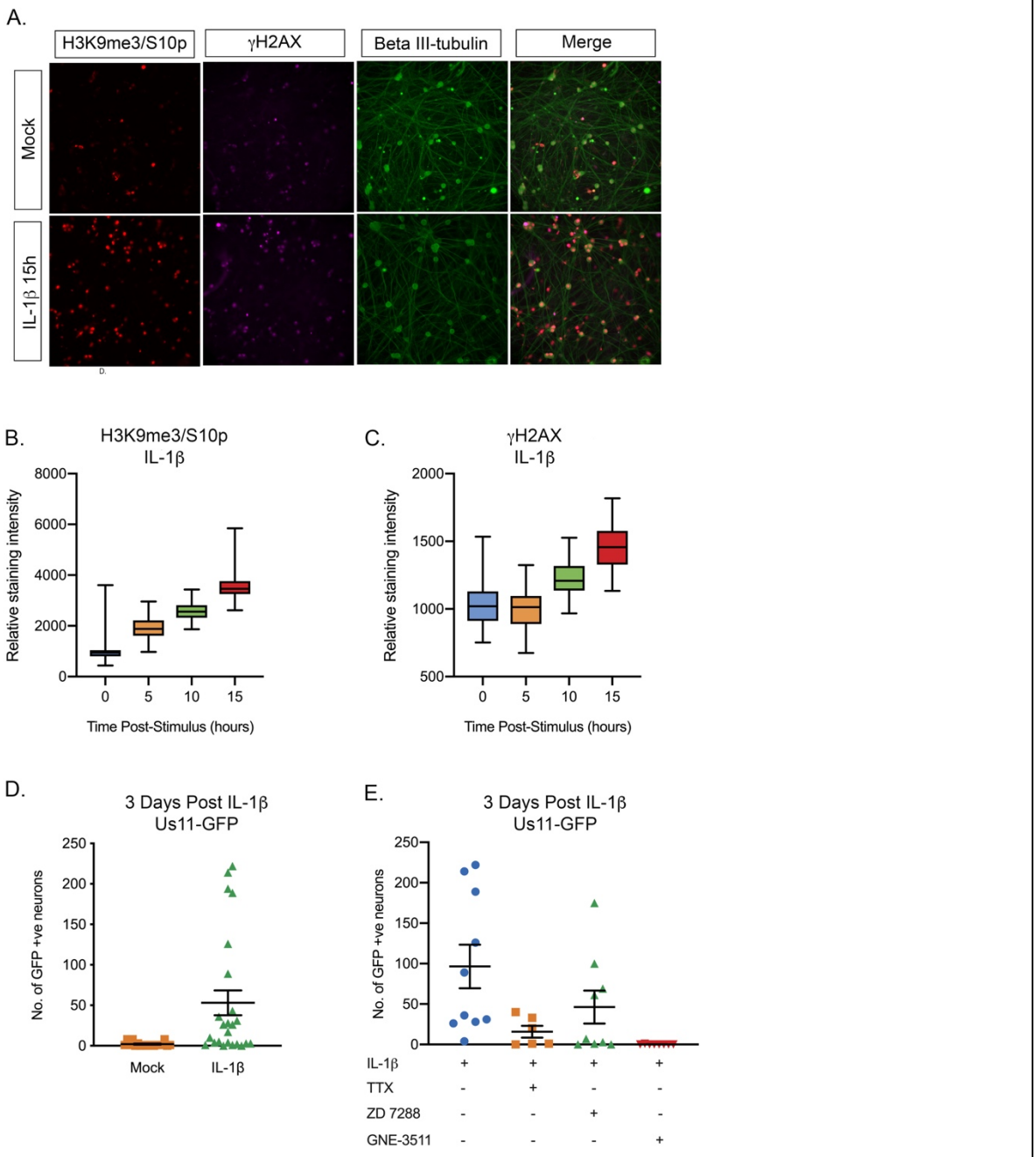

Figure 6

Figure 6. IL-1β-Induced HSV Reactivation is Linked to Heightened Neuronal Activity and DLK Activation. (A) Adult P28 SCG neurons were treated with IL-1β (30ng/mL) for 15 hrs and stained for H3K9me3/S10p, γH2AX and beta II-tubulin to mark neurons. (B-C) Quantification of the intensity of H3K9me3/S10p and γH2AX in neuronal nuclei following forskolin treatment from two independent experiments. (D). Addition of IL-1β to latently infected cultures of mature SCG neurons triggers HSV reactivation. (E). Quantification of IL-1β induced reactivation in the presence of the voltage gated sodium channel blocker TTX (1μM), the

HCN channel blocker ZD 7288 (10μM) and the DLK inhibitor GNE-3511 (4μM). In D and E individual experimental replicates are represented. Statistical comparisons were made using or two-tailed unpaired t-test (B, C) or Welch's t-test (D, E)

neuronal excitation as IL-1β increases the expression of voltage-gated sodium channels[40]. Importantly, IL-1β was able to trigger HSV reactivation in mature neurons (Figure 5D). Reactivation was reduced in the presence of the HCN-channel inhibitor ZD 7288 and the voltage-gated sodium channel inhibitor TTX (Figure 6F), indicating that IL-1β triggered reactivation via increasing neuronal activity. Importantly, addition of the DLK inhibitor GNE-3511 blocked reactivation in response to IL-1β (Figure 6F). Therefore, IL-1β can induce HSV reactivation that is both dependent on neuronal activity and induction of the JNK neuronal cell stress response.

Discussion

As herpesviruses hide in the form of a latent infections of specific cell types, they sense changes to the infected cell, resulting in the expression of viral lytic genes and ultimately reactivation. HSV establishes latency in neurons and has previously been found to respond to activation of a neuronal stress signaling pathway[15]. As an excitable cell type, the function of neurons is to rapidly transmit stimuli via the firing of action potentials, and under conditions of hyperexcitability, neurons increase their propensity to fire repeated action potentials. Here we show that this state of hyperexcitability induces HSV to undergo reactivation in a DLK/JNK dependent manner, indicating that the virus responds to both activation of cell stress signaling and prolonged hyperexcitability via a common pathway to result in reactivation. This common pathway also permits viral lytic gene expression from silenced promoters without the requirement

of histone demethylase activity via a histone phospho/methyl switch. Conditions that result in hyperexcitability include prolonged periods of stress and inflammation, which are both linked to the release of IL-1β[31-34]. Consistent with this, here we show that IL-1β induces DNA damage, and histone H3 phosphorylation in sympathetic neurons, which are both markers of neuronal excitability. Importantly, IL-1β triggered HSV reactivation that was dependent on neuronal activity and activation of DLK. Therefore, this study identifies a physiological stimulus that induces HSV reactivation via increasing neuronal excitability and places DLK/JNK signaling and a histone phospho/methyl switch as central to HSV reactivation.

Neuronal hyperexcitability results in DNA damage followed by repair, which together are thought to mediate the expression of cellular immediate early genes[29,30]. Here we show that forskolin treatment and IL-1β also induce DNA damage in sympathetic neurons. Previously, HSV reactivation has been found to occur following inhibition of DNA damage, inhibition of repair and exogenous DNA damage[12]. In the context of repair inhibition or exogenous DNA damage, reactivation was dependent on dephosphorylation of AKT by the PHLPP1 phosphatase and activation of JNK, and therefore feeds into the same pathway as PI3K-inhibition. However, we did not observe decreased AKT phosphorylation in response to forskolin treatment, indicating that the mechanism of reactivation is distinct following physiological levels of DNA damage resulting from neuronal hyperexcitability versus perturbation of the damage/repair pathways.

Conditions that result in hyperexcitability include prolonged periods of stress and inflammation, which are both linked to the release of IL-1β[31-34]. Consistent with these findings, we show that IL-1β treatment induces two markers of neuronal excitability, DNA damage and histone H3 phosphorylation, in primary sympathetic neurons. The IL-1 family of cytokines act via the IL-1 receptor to activate downstream signaling pathways [64]. IL-1β is released systemically during prolonged periods of psychological stress and upon infection via activation of the inflammasome[31-34]. IL-1α, which also signals via the IL-1R, is released locally as an alarmin. Interesting IL-1α and IL-1β are found at high levels in keratinocytes and are released upon HSV-1 infection[41], where they can mediate antiviral responses in underlying stromal fibroblasts and endothelial cells. Antiviral responses mediated by IL-1 signaling have been found to involve NF-κB, IRF3 and/or IRF1[42]. The downstream signaling elicited by IL-1 in neurons has not been clearly defined and likely varies between different subtypes of neurons. NF-κB has been reported to be absent in certain subtypes of neurons but constitutively active in others[65,66], and a recent study suggests that NF-κB levels increase with neuronal maturation[67], which may be why we only observed IL-1-mediated reactivation in mature neurons. Additional studies have found a role for p38MAPK signaling and AKT/mTOR signaling in neuronal IL-1-mediated responses[68,69]. A common feature of IL-1 signaling in neurons is increased excitability, which has been associated with neurotransmitter release, and mediates a variety of physiological responses including behavior modulation and an intersection with the hosts' immune response[38-40]. IL-1 is also associated with pathological conditions, including neurodegenerative disease such as Alzheimer's disease[70]. There are multiple studies linking HSV-1 infection to the

461 progression of Alzheimer's[2]; therefore, the combination of both HSV infection and
462 increased IL-1 could have a feed forward effect on the progression of Alzheimer's
463 disease by promoting increased reactivation of HSV from latency.
464
465 Experiments using primary neuronal *in vitro* model systems and inducing
466 reactivation by PI3-kinase inhibition have shown that reactivation progresses over two
467 phases. Phase 1 involves the synchronous up-regulation of lytic gene expression that
468 occurs independently of the viral transactivator VP16 and the activity of cellular histone
469 demethylases[15,18]. A population of neurons progress to full reactivation (Phase II), which
470 is dependent on both VP16 and HDM activity[15,18]. We previously found that lytic gene
471 expression in Phase I is DLK/JNK dependent and is corelated with a JNK-dependent
472 histone methyl/phospho switch on lytic gene promoters[15]. Here we demonstrate that a
473 Phase 1 wave of viral gene expression that is dependent on activation of JNK but not
474 histone demethylases also occurs in response to neuronal hyperexcitability. The co-
475 localization of viral genomes with H3K9me3/pS10 indicates that a histone
476 methyl/phospho switch also permits lytic gene expression to occur following forskolin
477 treatment in a manner that is independent of HDM activity. This indicates that
478 reactivation proceeds via a Phase 1-wave of gene expression in response to multiple
479 different stimuli. However we note that there may be differences in the mechanism and
480 kinetics of reactivation with different stimuli and/or strains of HSV-1 as reactivation
481 triggered by axotomy may bypass Phase I[19,20] and reactivation induced in vivo by heat
482 shock with a more pathogenic strain of HSV triggered more rapid reactivation [71]. It will
483 be especially interesting to determine in the future whether there are differences in the

484 progression to reactivation with different strains of HSV. Ultimately, these reactivation
485 kinetics may relate differences in the epigenetic structures of viral genomes that vary
486 based on virus strains or differential manipulation of host-cell signaling pathways.
487
488 The Wilcox lab demonstrated in 1992 that reactivation can be induced by
489 forskolin, and it has since been used as a trigger in multiple studies[25-28]. However, the
490 mechanism by which increasing levels of cAMP induces lytic gene expression was not
491 known. Here we link cAMP-induced reactivation to the excitation state of the neuron and
492 show that the initial induction of viral gene expression is dependent on DLK and JNK
493 activity but independent of CREB and PKA. The activity of PKA may be required for full
494 reactivation, which is also consistent with a role for PKA in overcoming repression of the
495 related Pseudorabies Virus during *de novo* axonal infection[72]. Our data also suggest
496 that CREB may be involved in the progression to full reactivation. However, the
497 mechanism of action of the inhibitor used here, 666-15, is not entirely clear. It has been
498 reported as preventing CREB-mediated gene expression, but may act to prevent
499 recruitment of histone acetyltransferases[73]. Therefore, inhibition of Phase II reactivation
500 by 666-15 would be consistent with more large-scale chromatin remodeling on the viral
501 genome at this stage. In addition, previous work has identified a role for inducible cAMP
502 early repressor (ICER) in HSV reactivation[26]. ICER is a repressor of gene expression
503 via heterodimerization with members of the CREB/ATF family of transcription factors.
504 CREB expression is also known to be down-regulated by loss of NGF-signaling[74].
505 Therefore, it is conceivable that inhibition, rather than activation, of CREB is important
506 for reactivation of HSV from latency.

Previously, we found that JNK activation by DLK is required for reactivation following interruption of the NGF-signaling pathway. Here we find that forskolin and IL-1β-mediated reactivation also required both DLK activity, further reinforcing the central role of DLK and JNK in reactivation of HSV from latency. DLK is known as a master regulator of neuronal response to stress stimuli and mediates whole cell death, axon pruning, regeneration or generation depending on the nature of the stimuli. However, it has not before been linked to neuronal hyperexcitability or the response to IL-1β signaling. The known mechanisms of DLK activation include loss of AKT activation and phosphorylation by PKA, neither of which could be linked to HSV reactivation mediated by forskolin in this study. Following activation by DLK, one mechanism by which JNK is thought to permit lytic gene expression is via recruitment to viral promoters and histone phosphorylation. However, it is likely that there are additional, JNK-dependent effects including activation of pioneer or transcription factors that also mediate viral gene expression. Further insight into how HSV has hijacked this cellular pathway to induce lytic gene expression may lead to novel therapeutics that prevent reactivation, in addition to providing information on how viral gene expression initiates from promoters assembled into heterochromatin.

Acknowledgements

We thank Ian Mohr (NYU) for supplying the Us11-GFP virus used in this study. This work was supported by NIH/NINDS R01NS105630 (to A.R.C), NIH/NIAID T32AI007046

(S.R.C. and J.B.S), NIH/NEI F30EY030397 (J.B.S), NIH/NIGMS T32GM008136 (S.D) and T32GM007267 (J.B.S) and MRC (https://mrc.ukri.org) MC_UU_12014/5 (C.B).

Materials and Methods

Reagents

Compounds used in the study are as follows: Acycloguanosine, FUDR, Uridine, SP600125, GNE-3511, GSK-J4, L-Glutamic Acid, and Ivabradine (Millipore Sigma); Forskolin, LY 294002, 666-15, SQ 22536, KT 5720, Tetraethylammonium chloride, Cesium chloride, OG-L002, S2101, Tetrotdotoxin, and ESI-09 (Tocris); 1,9-dideoxy Forskolin, ZD 7288 and 8-bromo-cyclic AMP (Cayman Chemicals); Nerve Growth Factor 2.5S (Alomone Labs); Primocin (Invivogen); Aphidicolin (AG Scientific); IL-1β (Shenandoah Biotechnology); WAY-150138 was kindly provided by Pfizer, Dr. Jay Brown and Dr. Dan Engel at the University of Virginia, and Dr. Lynn Enquist at Princeton University. Compound information and concentrations used can be found below in Table S1.

Preparation of HSV-1 Virus Stocks

HSV-1 stocks of eGFP-Us11 Patton were grown and titrated on Vero cells obtained from the American Type Culture Collection (Manassas, VA). Cells were maintained in Dulbecco's Modified Eagle's Medium (Gibco) supplemented with 10% FetalPlex (Gemini Bio-Products) and 2 mM L-Glutamine. eGFP-Us11 Patton (HSV-1 Patton strain with eGFP reporter protein fused to true late protein Us11[43]) was kindly provided by Dr. Ian Mohr at New York University.

552

553 **Primary Neuronal Cultures**

554 Sympathetic neurons from the Superior Cervical Ganglia (SCG) of post-natal day 0-2
555 (P0-P2) or adult (P21-P24) CD1 Mice (Charles River Laboratories) were dissected as
556 previously described[15]. Rodent handling and husbandry were carried out under animal
557 protocols approved by the Animal Care and Use Committee of the University of Virginia
558 (UVA). Ganglia were briefly kept in Leibovitz's L-15 media with 2.05 mM L-Glutamine
559 before dissociation in Collagenase Type IV (1 mg/mL) followed by Trypsin (2.5 mg/mL)
560 for 20 minutes each at 37 ˚C. Dissociated ganglia were triturated, and approximately
561 10,000 neurons per well were plated onto rat tail collagen in a 24-well plate.
562 Sympathetic neurons were maintained in CM1 (Neurobasal® Medium supplemented
563 with PRIME-XV IS21 Neuronal Supplement (Irvine Scientific), 50 ng/mL Mouse NGF
564 2.5S, 2 mM L-Glutamine, and Primocin). Aphidicolin (3.3 µg/mL), Fluorodeoxyuridine
565 (20 µM) and Uridine (20 µM) were added to the CM1 for the first five days post-
566 dissection to select against proliferating cells.

567

568 **Establishment and Reactivation of Latent HSV-1 Infection in Primary Neurons**

569 Latent HSV-1 infection was established in P6-8 sympathetic neurons from SCGs.
570 Neurons were cultured for at least 24 hours without antimitotic agents prior to infection.
571 The cultures were infected with eGFP-Us11 (Patton recombinant strain of HSV-1
572 expressing an eGFP reporter fused to true late protein Us11). Neurons were infected at
573 a Multiplicity of Infection (MOI) of 7.5 PFU/cell (assuming $1.0x10^4$ neurons/well/24-well
574 plate) in DPBS +$CaCl_2$ +$MgCl_2$ supplemented with 1% Fetal Bovine Serum, 4.5 g/L

glucose, and 10 μM Acyclovir (ACV) for three hours at 37 ˚C. Post-infection, inoculum was replaced with CM1 containing 50 μM ACV for 5-6 days, followed by CM1 without ACV. Reactivation was carried out in DMEM/F12 (Gibco) supplemented with 10% Fetal Bovine Serum, Mouse NGF 2.5S (50 ng/mL) and Primocin. Inhibitors were added either one hour prior to or concurrently with the reactivation stimulus. WAY-150138 (2-10 μg/mL) was added to reactivation cocktail to limit cell-to-cell spread. Reactivation was quantified by counting number of GFP-positive neurons or performing Reverse Transcription Quantitative PCR (RT-qPCR) of HSV-1 lytic mRNAs isolated from the cells in culture.

Analysis of mRNA expression by reverse-transcription quantitative PCR (RT-qPCR)

To assess relative expression of HSV-1 lytic mRNA, total RNA was extracted from approximately $1.0x10^4$ neurons using the Quick-RNA™ Miniprep Kit (Zymo Research) with an on-column DNase I digestion. mRNA was converted to cDNA using the SuperScript IV First-Strand Synthesis system (Invitrogen) using equal amounts of RNA (20-30 ng/reaction). To assess viral DNA load, total DNA was extracted from approximately $1.0x10^4$ neurons using the Quick-DNA™ Miniprep Plus Kit (Zymo Research). qPCR was carried out using *Power* SYBR™ Green PCR Master Mix (Applied Biosystems). The relative mRNA or DNA copy number was determined using the Comparative C_T ($\Delta\Delta C_T$) method normalized to mRNA or DNA levels in latently infected samples. Viral RNAs were normalized to mouse reference gene GAPDH. All

samples were run in duplicate on an Applied Biosystems™ QuantStudio™ 6 Flex Real-Time PCR System. Primers used are described in Table S2.

Western Blot Analysis

Neurons were lysed in RIPA Buffer with cOmplete, Mini, EDTA-Free Protease Inhibitor Cocktail (Roche) and PhosSTOP Phosphatase Inhibitor Cocktail (Roche) on ice for one hour with regular vortexing to aid lysis. Insoluble proteins were removed via centrifugation, and lysate protein concentration was determined using the Pierce Bicinchoninic Acid Protein Assay Kit (Invitrogen) using a standard curve created with BSA standards of known concentration. Equal quantities of protein (generally 20-50 µg) were resolved on 4-20% gradient SDS-Polyacrylamide gels (Bio-Rad) and then transferred onto Polyvinylidene difluoride membranes (Millipore Sigma). Membranes were blocked in PVDF Blocking Reagent for Can Get Signal (Toyobo) for one hour. Primary antibodies were diluted in Can Get Signal Immunoreaction Enhancer Solution 1 (Toyobo) and membranes were incubated overnight at 4^{o}C. Antibodies and concentrations are described in Table S3 below. HRP-labeled secondary antibodies were diluted in Can Get Signal Immunoreaction Enhancer Solution 2 (Toyobo) and membranes were incubated for one hour at room temperature. Blots were developed using Western Lightning Plus-ECL Enhanced Chemiluminescence Substrate (PerkinElmer) and ProSignal ECL Blotting Film (Prometheus Protein Biology Products) according to manufacturer's instructions. Blots were stripped for reblotting using NewBlot PVDF Stripping Buffer (Licor).

620 **Immunofluorescence**

621 Neurons were fixed for 15 minutes in 4% Formaldehyde and blocked in 5% Bovine
622 Serum Albumin and 0.3% Triton X-100 and incubated overnight in primary antibody.
623 Antibodies and concentrations are described in Table S4 below. Following primary
624 antibody treatment, neurons were incubated for one hour in Alexa Fluor® 488-, 555-,
625 and 647-conjugated secondary antibodies for multi-color imaging (Invitrogen). Nuclei
626 were stained with Hoechst 33258 (Life Technologies). Images were acquired using an
627 sCMOS charge-coupled device camera (pco.edge) mounted on a Nikon Eclipse Ti
628 Inverted Epifluorescent microscope using NIS-Elements software (Nikon). Images were
629 analyzed and intensity quantified using ImageJ.

630

631 **Click Chemistry**

632 Click chemistry was carried out a described previously[52] with some modifications.
633 Neurons were washed with CSK buffer (10 mM HEPES, 100 mM NaCl, 300 mM
634 Sucrose, 3 mM $MgCl_2$, 5 mM EGTA) and simultaneously fixed and permeabilized for 10
635 minutes in 1.8% methonal-free formaldehyde (0.5% Triton X-100, 1%
636 phenylmethylsulfonyl fluoride (PMSF)) in CSK buffer, then washed twice with PBS
637 before continuing to the click chemistry reaction and immunostaining. Samples were
638 blocked with 3% BSA for 30 minutes, followed by click chemistry using EdC-labelled
639 HSV-1 DNA and the Click-iT EdU Alexa Flour 555 Imaging Kit (ThermoFisher Scientific,
640 C10638) according to the manufacturer's instructions. For immunostaining, samples
641 were incubated overnight with primary antibodies in 3% BSA. Following primary
642 antibody treatment, neurons were incubated for one hour in Alexa Fluor® 488-, 555-,

and 647-conjugated secondary antibodies for multi-color imaging (Invitrogen). Nuclei were stained with Hoechst 33258 (Life Technologies). Images were acquired at 60x using an sCMOS charge-coupled device camera (pco.edge) mounted on a Nikon Eclipse Ti Inverted Epifluorescent microscope using NIS-Elements software (Nikon). Images were analyzed and intensity quantified using ImageJ.

Statistical Analysis

Power analysis was used to determine the appropriate sample sizes for statistical analysis. All statistical analysis was performed using Prism V8.4. Welch's t-test was used for GFP fluorescence experiments and two-tailed unpaired t-test was used for RT-qPCR and IF experiments; specific analyses are included in the figure legends. EdC virus and H3K9me3S10/p co-localization was quantified using ImageJ after sample blinding. Mean fluorescence intensity of γH2AX was quantified using ImageJ.

References

1 Arvin, A. *et al.* Human Herpesviruses: Biology, Therapy, and Immunoprophylaxis. (2007).

2 Itzhaki, R. F. Corroboration of a Major Role for Herpes Simplex Virus Type 1 in Alzheimer's Disease. *Front Aging Neurosci* **10**, 324, doi:10.3389/fnagi.2018.00324 (2018).

3 Suzich, J. B. & Cliffe, A. R. Strength in diversity: Understanding the pathways to herpes simplex virus reactivation. *Virology* **522**, 81-91, doi:10.1016/j.virol.2018.07.011 (2018).

4 Deshmane, S. L. & Fraser, N. W. During latency, herpes simplex virus type 1 DNA is associated with nucleosomes in a chromatin structure. *J Virol* **63**, 943-947 (1989).

5 Wang, Q. Y. *et al.* Herpesviral latency-associated transcript gene promotes assembly of heterochromatin on viral lytic-gene promoters in latent infection. *Proc Natl Acad Sci U S A* **102**, 16055-16059, doi:10.1073/pnas.0505850102 (2005).

6 Knipe, D. M. & Cliffe, A. Chromatin control of herpes simplex virus lytic and latent infection. *Nat Rev Microbiol* **6**, 211-221, doi:10.1038/nrmicro1794 (2008).

7 Cliffe, A. R., Garber, D. A. & Knipe, D. M. Transcription of the herpes simplex virus latency-associated transcript promotes the formation of facultative heterochromatin on lytic promoters. *J Virol* **83**, 8182-8190, doi:10.1128/JVI.00712-09 (2009).

8 Kwiatkowski, D. L., Thompson, H. W. & Bloom, D. C. The polycomb group protein Bmi1 binds to the herpes simplex virus 1 latent genome and maintains repressive histone marks during latency. *J Virol* **83**, 8173-8181, doi:10.1128/JVI.00686-09 (2009).

9 Wilcox, C. L. & Johnson, E. M., Jr. Characterization of nerve growth factor-dependent herpes simplex virus latency in neurons in vitro. *J Virol* **62**, 393-399 (1988).

10 Wilcox, C. L., Smith, R. L., Freed, C. R. & Johnson, E. M., Jr. Nerve growth factor-dependence of herpes simplex virus latency in peripheral sympathetic and sensory neurons in vitro. *J Neurosci* **10**, 1268-1275 (1990).

11 Camarena, V. *et al.* Nature and duration of growth factor signaling through receptor tyrosine kinases regulates HSV-1 latency in neurons. *Cell Host Microbe* **8**, 320-330, doi:10.1016/j.chom.2010.09.007 (2010).

12 Hu, H. L. *et al.* TOP2beta-Dependent Nuclear DNA Damage Shapes Extracellular Growth Factor Responses via Dynamic AKT Phosphorylation to Control Virus Latency. *Mol Cell* **74**, 466-480 e464, doi:10.1016/j.molcel.2019.02.032 (2019).

13 Tedeschi, A. & Bradke, F. The DLK signalling pathway--a double-edged sword in neural development and regeneration. *EMBO reports* **14**, 605-614, doi:10.1038/embor.2013.64 (2013).

14 Geden, M. J. & Deshmukh, M. Axon degeneration: context defines distinct pathways. *Curr Opin Neurobiol* **39**, 108-115, doi:10.1016/j.conb.2016.05.002 (2016).

15 Cliffe, A. R. *et al.* Neuronal Stress Pathway Mediating a Histone Methyl/Phospho Switch Is Required for Herpes Simplex Virus Reactivation. *Cell Host Microbe* **18**, 649-658, doi:10.1016/j.chom.2015.11.007 (2015).

16 Fischle, W. *et al.* Regulation of HP1–chromatin binding by histone H3 methylation and phosphorylation. *Nature* **438**, 1116-1122, doi:10.1038/nature04219 (2005).

17 Gehani, S. S. *et al.* Polycomb group protein displacement and gene activation through MSK-dependent H3K27me3S28 phosphorylation. *Mol Cell* **39**, 886-900, doi:10.1016/j.molcel.2010.08.020 (2010).

18 Kim, J. Y., Mandarino, A., Chao, M. V., Mohr, I. & Wilson, A. C. Transient reversal of episome silencing precedes VP16-dependent transcription during reactivation of latent HSV-1 in neurons. *PLoS Pathog* **8**, e1002540, doi:10.1371/journal.ppat.1002540 (2012).

19 Cliffe, A. R. & Wilson, A. C. Restarting Lytic Gene Transcription at the Onset of Herpes Simplex Virus Reactivation. *J Virol* **91**, e01419-01416-01416, doi:10.1128/JVI.01419-16 (2017).

20 Liang, Y., Vogel, J. L., Narayanan, A., Peng, H. & Kristie, T. M. Inhibition of the histone demethylase LSD1 blocks alpha-herpesvirus lytic replication and reactivation from latency. *Nat Med* **15**, 1312-1317, doi:10.1038/nm.2051 (2009).

21 Liang, Y. *et al.* Targeting the JMJD2 histone demethylases to epigenetically control herpesvirus infection and reactivation from latency. *Sci Transl Med* **5**, 167ra165, doi:10.1126/scitranslmed.3005145 (2013).

22 Messer, H. G., Jacobs, D., Dhummakupt, A. & Bloom, D. C. Inhibition of H3K27me3-specific histone demethylases JMJD3 and UTX blocks reactivation of herpes simplex virus 1 in trigeminal ganglion neurons. *J Virol* **89**, 3417-3420, doi:10.1128/JVI.03052-14 (2015).

23 Hill, J. M. *et al.* Inhibition of LSD1 reduces herpesvirus infection, shedding, and recurrence by promoting epigenetic suppression of viral genomes. *Sci Transl Med* **6**, 265ra169, doi:10.1126/scitranslmed.3010643 (2014).

24 Noh, K. M. *et al.* ATRX tolerates activity-dependent histone H3 methyl/phos switching to maintain repetitive element silencing in neurons. *Proc Natl Acad Sci U S A* **112**, 6820-6827, doi:10.1073/pnas.1411258112 (2015).

25 Smith, R. L., Pizer, L. I., Johnson, E. M., Jr. & Wilcox, C. L. Activation of second-messenger pathways reactivates latent herpes simplex virus in neuronal cultures. *Virology* **188**, 311-318, doi:10.1016/0042-6822(92)90760-m (1992).

26 Colgin, M. A., Smith, R. L. & Wilcox, C. L. Inducible cyclic AMP early repressor produces reactivation of latent herpes simplex virus type 1 in neurons in vitro. *J Virol* **75**, 2912-2920, doi:10.1128/JVI.75.6.2912-2920.2001 (2001).

27 De Regge, N., Van Opdenbosch, N., Nauwynck, H. J., Efstathiou, S. & Favoreel, H. W. Interferon Alpha Induces Establishment of Alphaherpesvirus Latency in Sensory Neurons In Vitro. *PLoS ONE* **5**, e13076, doi:10.1371/journal.pone.0013076.t001 (2010).

28 Danaher, R. J., Jacob, R. J. & Miller, C. S. Herpesvirus quiescence in neuronal cells. V: forskolin-responsiveness of the herpes simplex virus type 1 alpha0 promoter and contribution of the putative cAMP response element. *J Neurovirol* **9**, 489-497, doi:10.1080/13550280390218797 (2003).

29 Alt, F. W. & Schwer, B. DNA double-strand breaks as drivers of neural genomic change, function, and disease. *DNA Repair (Amst)* **71**, 158-163, doi:10.1016/j.dnarep.2018.08.019 (2018).

30 Madabhushi, R. *et al.* Activity-Induced DNA Breaks Govern the Expression of Neuronal Early-Response Genes. *Cell* **161**, 1592-1605, doi:10.1016/j.cell.2015.05.032 (2015).

31 Ericsson, A., Kovacs, K. J. & Sawchenko, P. E. A functional anatomical analysis of central pathways subserving the effects of interleukin-1 on stress-related neuroendocrine neurons. *J Neurosci* **14**, 897-913, doi:10.1523/jneurosci.14-02-00897.1994 (1994).

32 Goshen, I. & Yirmiya, R. Interleukin-1 (IL-1): a central regulator of stress responses. *Front Neuroendocrinol* **30**, 30-45, doi:10.1016/j.yfrne.2008.10.001 (2009).

744 33 Koo, J. W. & Duman, R. S. Interleukin-1 receptor null mutant mice show decreased
745 anxiety-like behavior and enhanced fear memory. *Neurosci Lett* **456**, 39-43,
746 doi:10.1016/j.neulet.2009.03.068 (2009).
747 34 Saper, C. B. & Breder, C. D. The neurologic basis of fever. *N Engl J Med* **330**, 1880-1886,
748 doi:10.1056/NEJM199406303302609 (1994).
749 35 Glaser, R. & Kiecolt-Glaser, J. K. Chronic stress modulates the virus-specific immune
750 response to latent herpes simplex virus type 1. *Ann Behav Med* **19**, 78-82,
751 doi:10.1007/BF02883323 (1997).
752 36 Cohen, F. *et al.* Persistent stress as a predictor of genital herpes recurrence. *Arch Intern*
753 *Med* **159**, 2430-2436, doi:10.1001/archinte.159.20.2430 (1999).
754 37 Chida, Y. & Mao, X. Does psychosocial stress predict symptomatic herpes simplex virus
755 recurrence? A meta-analytic investigation on prospective studies. *Brain, behavior, and*
756 *immunity* **23**, 917-925, doi:10.1016/j.bbi.2009.04.009 (2009).
757 38 Vezzani, A. & Viviani, B. Neuromodulatory properties of inflammatory cytokines and
758 their impact on neuronal excitability. *Neuropharmacology* **96**, 70-82,
759 doi:10.1016/j.neuropharm.2014.10.027 (2015).
760 39 Schneider, H. *et al.* A neuromodulatory role of interleukin-1beta in the hippocampus.
761 *Proc Natl Acad Sci U S A* **95**, 7778-7783, doi:10.1073/pnas.95.13.7778 (1998).
762 40 Binshtok, A. M. *et al.* Nociceptors are interleukin-1beta sensors. *J Neurosci* **28**, 14062-
763 14073, doi:10.1523/JNEUROSCI.3795-08.2008 (2008).
764 41 Orzalli, M. H. *et al.* An Antiviral Branch of the IL-1 Signaling Pathway Restricts Immune-
765 Evasive Virus Replication. *Mol Cell* **71**, 825-840 e826, doi:10.1016/j.molcel.2018.07.009 (2018).
766 42 Aarreberg, L. D. *et al.* Interleukin-1beta Induces mtDNA Release to Activate Innate
767 Immune Signaling via cGAS-STING. *Mol Cell* **74**, 801-815 e806,
768 doi:10.1016/j.molcel.2019.02.038 (2019).
769 43 Benboudjema, L., Mulvey, M., Gao, Y., Pimplikar, S. W. & Mohr, I. Association of the
770 herpes simplex virus type 1 Us11 gene product with the cellular kinesin light-chain-related
771 protein PAT1 results in the redistribution of both polypeptides. *J Virol* **77**, 9192-9203,
772 doi:10.1128/jvi.77.17.9192-9203.2003 (2003).
773 44 Hoshi, T., Garber, S. S. & Aldrich, R. W. Effect of forskolin on voltage-gated K+ channels
774 is independent of adenylate cyclase activation. *Science* **240**, 1652-1655 (1988).
775 45 Kandel, E. R. The molecular biology of memory: cAMP, PKA, CRE, CREB-1, CREB-2, and
776 CPEB. *Mol Brain* **5**, 14, doi:10.1186/1756-6606-5-14 (2012).
777 46 de Rooij, J. *et al.* Mechanism of regulation of the Epac family of cAMP-dependent
778 RapGEFs. *J Biol Chem* **275**, 20829-20836, doi:10.1074/jbc.M001113200 (2000).
779 47 Gandia, L. *et al.* Differential effects of forskolin and 1,9-dideoxy-forskolin on nicotinic
780 receptor- and K+-induced responses in chromaffin cells. *Eur J Pharmacol* **329**, 189-199,
781 doi:https://doi.org/10.1016/S0014-2999(97)89180-7 (1997).
782 48 Haslam, R. J., Davidson, M. M. & Desjardins, J. V. Inhibition of adenylate cyclase by
783 adenosine analogues in preparations of broken and intact human platelets. Evidence for the
784 unidirectional control of platelet function by cyclic AMP. *Biochem J* **176**, 83-95,
785 doi:10.1042/bj1760083 (1978).

786 49 Patel, S. *et al.* Discovery of dual leucine zipper kinase (DLK, MAP3K12) inhibitors with
787 activity in neurodegeneration models. *J Med Chem* **58**, 401-418, doi:10.1021/jm5013984
788 (2015).
789 50 van Zeijl, M. *et al.* Novel class of thiourea compounds that inhibit herpes simplex virus
790 type 1 DNA cleavage and encapsidation: resistance maps to the UL6 gene. *J Virol* **74**, 9054-9061,
791 doi:10.1128/jvi.74.19.9054-9061.2000 (2000).
792 51 Newcomb, W. W. & Brown, J. C. Inhibition of herpes simplex virus replication by WAY-
793 150138: assembly of capsids depleted of the portal and terminase proteins involved in DNA
794 encapsidation. *J Virol* **76**, 10084-10088, doi:10.1128/jvi.76.19.10084-10088.2002 (2002).
795 52 Alandijany, T. *et al.* Distinct temporal roles for the promyelocytic leukaemia (PML)
796 protein in the sequential regulation of intracellular host immunity to HSV-1 infection. *PLoS*
797 *Pathog* **14**, e1006769, doi:10.1371/journal.ppat.1006769 (2018).
798 53 McFarlane, S. *et al.* The histone chaperone HIRA promotes the induction of host innate
799 immune defences in response to HSV-1 infection. *PLoS Pathog* **15**, e1007667,
800 doi:10.1371/journal.ppat.1007667 (2019).
801 54 Kruidenier, L. *et al.* A selective jumonji H3K27 demethylase inhibitor modulates the
802 proinflammatory macrophage response. *Nature* **488**, 404-408, doi:10.1038/nature11262
803 (2012).
804 55 Sartiani, L., Mannaioni, G., Masi, A., Novella Romanelli, M. & Cerbai, E. The
805 Hyperpolarization-Activated Cyclic Nucleotide-Gated Channels: from Biophysics to
806 Pharmacology of a Unique Family of Ion Channels. *Pharmacol Rev* **69**, 354-395,
807 doi:10.1124/pr.117.014035 (2017).
808 56 Kullmann, P. H. *et al.* HCN hyperpolarization-activated cation channels strengthen
809 virtual nicotinic EPSPs and thereby elevate synaptic amplification in rat sympathetic neurons. *J*
810 *Neurophysiol* **116**, 438-447, doi:10.1152/jn.00223.2016 (2016).
811 57 DiFrancesco, D. & Tortora, P. Direct activation of cardiac pacemaker channels by
812 intracellular cyclic AMP. *Nature* **351**, 145-147, doi:10.1038/351145a0 (1991).
813 58 Kase, D. & Imoto, K. The Role of HCN Channels on Membrane Excitability in the Nervous
814 System. *J Signal Transduct* **2012**, 619747, doi:10.1155/2012/619747 (2012).
815 59 Ibata, K., Sun, Q. & Turrigiano, G. G. Rapid synaptic scaling induced by changes in
816 postsynaptic firing. *Neuron* **57**, 819-826, doi:10.1016/j.neuron.2008.02.031 (2008).
817 60 Turrigiano, G. G., Leslie, K. R., Desai, N. S., Rutherford, L. C. & Nelson, S. B. Activity-
818 dependent scaling of quantal amplitude in neocortical neurons. *Nature* **391**, 892-896,
819 doi:10.1038/36103 (1998).
820 61 Lee, H. K. & Kirkwood, A. Mechanisms of Homeostatic Synaptic Plasticity in vivo. *Front*
821 *Cell Neurosci* **13**, 520, doi:10.3389/fncel.2019.00520 (2019).
822 62 Sokolova, I. V. & Mody, I. Silencing-induced metaplasticity in hippocampal cultured
823 neurons. *J Neurophysiol* **100**, 690-697, doi:10.1152/jn.90378.2008 (2008).
824 63 Emery, E. C., Young, G. T., Berrocoso, E. M., Chen, L. & McNaughton, P. A. HCN2 ion
825 channels play a central role in inflammatory and neuropathic pain. *Science* **333**, 1462-1466,
826 doi:10.1126/science.1206243 (2011).
827 64 Weber, A., Wasiliew, P. & Kracht, M. Interleukin-1 (IL-1) pathway. *Sci Signal* **3**, cm1,
828 doi:10.1126/scisignal.3105cm1 (2010).

829 65 Listwak, S. J., Rathore, P. & Herkenham, M. Minimal NF-kappaB activity in neurons.
830 *Neuroscience* **250**, 282-299, doi:10.1016/j.neuroscience.2013.07.013 (2013).
831 66 Kaltschmidt, B. & Kaltschmidt, C. NF-kappaB in the nervous system. *Cold Spring Harb*
832 *Perspect Biol* **1**, a001271, doi:10.1101/cshperspect.a001271 (2009).
833 67 Yeh, J. X., Park, E., Schultz, K. L. W. & Griffin, D. E. NF-kappaB Activation Promotes
834 Alphavirus Replication in Mature Neurons. *J Virol* **93**, e01071-01019, doi:10.1128/JVI.01071-19
835 (2019).
836 68 Qian, J. *et al.* Interleukin-1R3 mediates interleukin-1-induced potassium current increase
837 through fast activation of Akt kinase. *Proc Natl Acad Sci U S A* **109**, 12189-12194,
838 doi:10.1073/pnas.1205207109 (2012).
839 69 Srinivasan, D., Yen, J. H., Joseph, D. J. & Friedman, W. Cell type-specific interleukin-1beta
840 signaling in the CNS. *J Neurosci* **24**, 6482-6488, doi:10.1523/JNEUROSCI.5712-03.2004 (2004).
841 70 Mrak, R. E. & Griffin, W. S. Interleukin-1, neuroinflammation, and Alzheimer's disease.
842 *Neurobiol Aging* **22**, 903-908, doi:10.1016/s0197-4580(01)00287-1 (2001).
843 71 Doll, J. R., Hoebe, K., Thompson, R. L. & Sawtell, N. M. Resolution of herpes simplex virus
844 reactivation in vivo results in neuronal destruction. *PLoS Pathog* **16**, e1008296,
845 doi:10.1371/journal.ppat.1008296 (2020).
846 72 Koyuncu, O. O., MacGibeny, M. A., Hogue, I. B. & Enquist, L. W. Compartmented
847 neuronal cultures reveal two distinct mechanisms for alpha herpesvirus escape from genome
848 silencing. *PLoS Pathog* **13**, e1006608, doi:10.1371/journal.ppat.1006608 (2017).
849 73 Xie, F. *et al.* Identification of a Potent Inhibitor of CREB-Mediated Gene Transcription
850 with Efficacious in Vivo Anticancer Activity. *J Med Chem* **58**, 5075-5087,
851 doi:10.1021/acs.jmedchem.5b00468 (2015).
852 74 Riccio, A., Ahn, S., Davenport, C. M., Blendy, J. A. & Ginty, D. D. Mediation by a CREB
853 family transcription factor of NGF-dependent survival of sympathetic neurons. *Science* **286**,
854 2358-2361 (1999).
855

856

857

858

859

860

861

862

863

864

Supplemental Tables of Reagents

Table S1: Compounds Used and Concentrations

Compound	Supplier	Identifier	Concentration
Acycloguanosine	Millipore Sigma	A4669	10 μM, 50 μM
FUDR	Millipore Sigma	F-0503	20 μM
Uridine	Millipore Sigma	U-3003	20 μM
SP600125	Millipore Sigma	S5567	20 μM
GNE-3511	Millipore Sigma	533168	4 μM
GSK-J4	Millipore Sigma	SML0701	2 μM
L-Glutamic Acid	Millipore Sigma	G5638	3.7 μg/mL
Forskolin	Tocris	1099	60 μM
LY 294002	Tocris	1130	20 μM
666-15	Tocris	5661	2 μM
SQ 22,536	Tocris	1435	50 μM
KT 5720	Tocris	1288	3 μM
TEA	Tocris	3068	10 mM
CsCl	Tocris	4739	3 mM
OG-L002	Tocris	6244	15 μM, 30 μM
S2101	Tocris	5714	10 μM, 20 μM
Tetrodotoxin	Tocris	1069	1 μM
ESI-09	Tocris	4773	10 μM
ZD 7288	Cayman	15228	20 μM
8-bromo-cyclic AMP	Cayman	14431	125 μM

NGF 2.5S	Alomone Labs	N-100	50 ng/mL
Primocin	Invivogen	ant-pm-1	100 µg/mL
Aphidicolin	AG Scientific	A-1026	3.3 µg/mL
IL-1β	Shenandoah Bio.	100-167	30ng/mL
WAY-150138	Pfizer	NA	10 µg/mL

867

868

869 Table S2: Primers Used for RT-qPCR

870

Primer	Sequence 5' to 3'
mGAP 1SF	CAT GGC CTT CCG TGT GTT CCT A
mGAP 1SR	GCG GCA CGT CAG ATC CA
ICP27 F	GCA TCC TTC GTG TTT GTC ATT CTG
ICP27 R	GCA TCT TCT CTC CGA CCC CG
ICP8 1SF	GGA GGT GCA CCG CAT ACC
ICP8 1SR	GGC TAA AAT CCG GCA TGA AC
ICP4 F	TGC TGC TGC TGT CCA CGC
ICP4 R	CGG TGT TGA CCA CGA TGA GCC
UL30 F	CGC GCT TGG CGG GTA TTA ACA T
UL30 R	TGG GTG TCC GGC AGA ATA AAG C

UL48 F	TGC TCG CGA ATG TGG TTT AG
UL48 R	CTG TTC CAG CCC TTC ATG TT
gC #1 F	GAG TTT GTC TGG TTC GAG GAC
gC #1R	ACG GTA GAG ACT GTG GTG AA

871

872

873 Table S3: Antibodies Used for Western Blotting and Concentrations

874

Antibody	Supplier	Identifier	Concentration
Rb Phospho-Akt (S473)	CST	4060	1:500
Rb Akt (pan)	CST	C67E7	1:1000
Rb Phospho-c-Jun (S73)	CST	3270	1:500
Ms Monoclonal α-Tubulin	Millipore Sigma	T9026	1:2500
HRP Goat Anti-Rabbit IgG Antibody (Peroxidase)	Vector	PI-1000	1:10000
HRP Horse Anti-Mouse IgG Antibody (Peroxidase)	Vector	PI-2000	1:10000

875

876

877 Table S4: Antibodies Used for Immunofluorescence and Concentrations

878

Antibody	Supplier	Identifier	Concentration
Rb H3K9me3S10P	Abcam	ab5819	1:250
Ch Beta-III Tubulin	Millipore sigma	AB9354	1:1000
Ms γH2A.X	CST	80312S	1:100
Ms c-Fos	Novus	NB110-75039	1:125
F(ab')2 Goat anti Mouse IgG (H+L) Alexa Fluor® 647	Thermo Fisher	A21237	1:1000
F(ab') Goat anti Rabbit IgG (H+L) Alexa Fluor® 555	Thermo Fisher	A21425	1:1000
Goat anti Chicken IgY (H+L) Alexa Fluor® 647	abcam	ab150175	1:1000
Goat Anti-Chicken IgY H&L (Alexa Fluor® 488) preabsorbed	abcam	ab150173	1:1000
F(ab')2 Goat anti-Rabbit IgG (H+L) Alexa Fluor® 488)	Thermo Fisher	B40922	1:1000

879

880

881

882